Feasibility assessment of newly isolated calcifying bacterial strains in self-healing concrete

Nafeesa Shaheen [a,b], Rao Arsalan Khushnood [a,*], Shazim Ali Memon [c], Fazal Adnan [d]

[a] *NUST Institute of Civil Engineering (NICE), School of Civil and Environmental Engineering (SCEE), National University of Sciences and Technology (NUST), Sector H-12, Islamabad 44000, Pakistan*
[b] *Department of Civil Engineering, Capital University of Science & Technology (CUST), Islamabad, Pakistan*
[c] *Department of Civil and Environmental Engineering, School of Engineering and Digital Sciences, Nazarbayev University, Astana, Kazakhstan*
[d] *Atta-ur-Rahman School of Applied Biosciences (ASAB), National University of Sciences and Technology (NUST), Sector H-12, Islamabad 44000, Pakistan*

ARTICLE INFO

ABSTRACT

In the present study, rarely explored spore former (*Bacillus safensis & Bacillus pumilus)* and non-spore former (*Arthrobacter luteolus, Chryseomicrobium imtechense & Corynebacterium efficiens)* alkaliphilic calcifying microbes were evaluated for their prolonged survival in cementitious environment. Extensive experimental program was designed to examine mechanical, self-healing, microstructural modifications and durability of self-healing concrete (SHC). Results of the experimental program endorsed the survival of all bacterial strains in the harsh concrete environment along-with improved mechanical response of matrix. Moreover, investigated strains were capable of precipitating copious amount of calcite having maximum of 0.8 mm average crack healing with 86 % strength recovery. Densification of microstructure was evident from the microstructural evaluation and pore refinement. SHC portrayed a significant resistance of 50 % and 20 % against Cl⁻ penetration and sulphate attack. Conclusively, these strains have potential to impart sustainability in concrete structures by extending the structural life, subsiding repairs cost and conserving the natural resources.

1. Introduction

Cement, a precursor of concrete composites, is the second largest consumed material on the planet after water. Its manufacturing is depleting the natural resources in addition to anthropogenic emissions into the environment [1]. Cracks and fissures, formed due to various natural or human activities are detrimental to the concrete structure and must be immediately repaired [2]. The repair of these unavoidable cracks is labor intensive and requires persistent monitoring [3]. To avoid these external interventions following the repairs, intrinsic self-repairing concrete system has been recommended [4,5].

At present, self-healing concrete via intrusion of calcifying microbes is designed to impart self-remediating properties inside the cementitious matrix [5,6]. This bio-influenced healing system plugs the pores by recurring microbially induced calcite precipitation (MICP) whereas healing process halts in other systems owing to depletion of healing agent [7]. Hence, the repairing efficiency of bio-influenced healing system depends on MICP that is itself linked with bacterial strain, precipitation pathway, nutrients availability and pH of the system [8]. Moreover, the addition of microbes into concrete system had also been found to enhance the mechanical properties of matrix against abrasion [9].

Survival inside high alkaline environment of concrete (internal pH up to 13) is a key factor for employment of heterotrophic soil bacterial namely *Bacillus, Pseudomonas, Sporosarcina, Shewanella* and *Echerichia* in the cementitious systems [8,10,11]. The optimum pH of calcite precipitation of previously practiced *Bacillus Subtilis (B. Subtilis), B. Sphaericus* and *Echerichia. Coli* is around 8 while concrete's internal pH is 13 [12–14]. Likewise *Sp. pasteurii* pH endurance is 10 but optimum calcite rate was observed at pH 7 [15]. Similarly, *B. cohnii, B. pseudofirmus* and
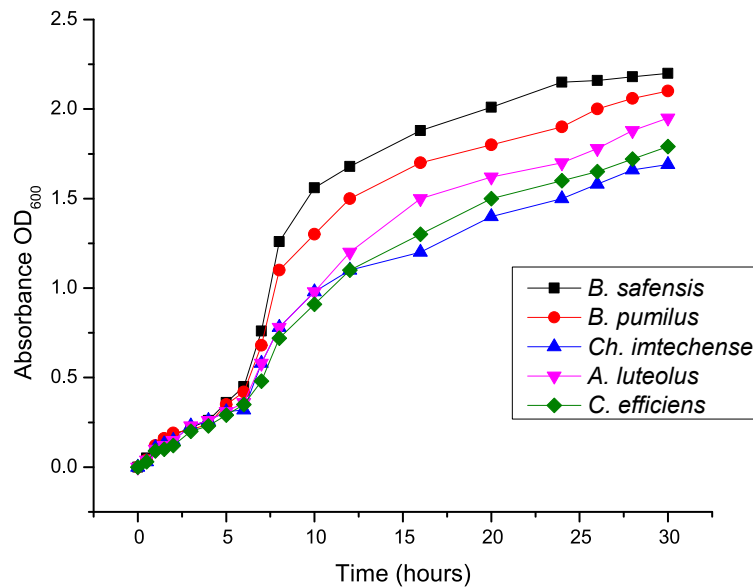

Fig. 1. Growth curves of investigated strains.

B. Cereus can survive at pH 10 but no data has been reported yet about their optimal calcite precipitation rate at this high alkaline pH [15–17]. Prevalence of *Bacillus* species is observed in SHC owing to their spore forming ability [18,19]. Besides inducing calcite precipitation, bacteria provide sites for nucleation [20]. The negatively charged cell walls of bacteria attracts the Ca^+ ions present in surroundings to stimulate the precipitation of calcite [21]. These bacteria precipitate calcite via passive and active pathways [22]. The commonly practiced passive pathway degrades the urea, which is detrimental for the environment and concrete [23–25]. Whereas, active pathway oxidizes the organic carbon, which is sustainable due to non-formation of toxic ammonia [23].

The precipitation rate of calcite is stimulated by the alkaline pH of the system whereas decrease in pH inhibits the calcite deposition [26,27]. However, the highly alkaline pH of the concrete system terminates the calcite deposition reaction by subsequently killing the microbes [28]. For proactive survival of microbes in alkaline environment, immobilization of microbes has been suggested [4,29,30]. Researchers investigated different immobilizers for enhancing the survival of microbes inside the concrete namely light weight aggregates (LWA), microcapsules, recycled aggregates (RCA), iron oxide, hydrogels, expanded perlite, zeolite etc. [31]. Among all, hydrogels and LWA aggregates showed promising results for healing [32,33]. However, they degraded the concrete properties besides additional cost [8,34]. In order to reduce the drawbacks of immobilization, alkaline pH resistant calcifying bacterial species are required having the potential to survive without immobilization.

Literature review inferred the lack of published research about alkaliphilic species having capabilities to produce abundant amount of calcite within the cementitious environment via active pathway without immobilization. Therefore, it is necessary to explore different types of calcifying bacterial species for their prolonged survival in the cementitious system [35]. In the present research, newly identified calcifying bacterial strains having potential to precipitate calcite at high pH via sustainable active pathway were used as healing agent [36]. These strains belonged to four diverse groups namely *Arthrobacter, Chryseomicrobium, Corynebacterium* and *Bacillus. Bacillus Species* are extensively researched in self-healing concrete; however, isolated strains have not been reported yet in SHC. Moreover, there is a lack of publicized literature about using *Arthrobacter, Chryseomicrobium* and *Corynebacterium species* in conjunction to self-healing cementitious systems. Therefore, the viability of these isolated strain was accessed via mechanical,

healing, microstructural and durability testing. To check any detrimental effect of these strains on concrete properties, mechanical analysis was performed in terms of compressive strength and split tensile strength. Self-healing potential was monitored via healed crack widths, regain in ultrasonic pulse velocity (UPV) and compressive strength values. Later on, healing precipitates were characterized using chemical and graphical modes of forensic assessment. Further, microstructure of hardened concrete matrix was examined through Brunauer-Emmett-Teller (BET), scanning electron microscopy (SEM), X-ray diffraction techniques (XRD) and thermal gravimetry (TG). Durability assessment of bio-influenced concrete was also performed using sorptivity, chloride ion migration and sulphate attack.

2. Materials and methods

2.1. Isolation and germination of microorganism

Alkaliphilic calcifying strains were isolated from industrial soils using enrichment media LB broth (5 yeast extract, 10 NaCl, 10 Tryptone) g/l having pH10. The pH of the media was adjusted using 2 N NaOH. For purification of distinct colonies, streaking was done repeatedly according to established protocols on LB agar plate media (5 yeast extract, 10 NaCl, 10 Tryptone, 15 agar) g/l having pH10 [37]. In order to identify the calcifying ability of isolated strains, $CaCO_3$ precipitation media (CPM) agar (80 calcium lactate, 4 yeast extract, 15 agar) g/l at pH10 was used. After phenetic analysis, distinct morphological microbes were subjected to DNA extraction and purification. Then, polymerase chain reaction (PCR) was performed and amplified *16S rRNA gene* was sequenced. Resulted sequences were uploaded on NCBI website to acquire accession number via Basic Local Alignment Search Tool (BLAST). High endurance calcifying strains were identified as *Bacillus Safensis* MUGA 156 *(Ac#MN865802), Bacillus pumilus SH-B9 (Ac#MN865840), Arthrobacter luteolus LNR3 (Ac#MN865845), Chryseomicrobium imtechense HTHB4 (Ac#MN867026)* and *Corynebacterium efficiens YS-314 (Ac# MN865795).* These isolated identified strains were able to survive in harsh alkaline environment [36].They are all gram-positive microbes having peptidoglycan layer commonly found in soil microbes. *Bacillus Safensis (B. safensis)* and *Bacillus pumilus (B. pumilus)* are rod shaped spore-formers bacteria. Whereas, *Arthrobacter luteolus (A. luteolus)* and *Corynebacterium efficiens (C. efficiens)* are cocci shaped non-spore-formers [38–40]. Likewise, *Chryseomicrobium imtechense (Chr.imtechense)* is non-spore-former and can be rod-shaped and coccus

Table 1

The physical and chemical properties of OPC.

CaO	SiO$_2$	Al$_2$O$_3$	Fe$_2$O	SO$_3$	MgO	K2O + Na$_2$O	LOI	Specific gravity	D$_{50}$ (um)	Blain fineness (cm^2/g)
63.35	20.35	4.87	3.26	2.71	2.41	0.58	3.84	3.17	6.57	3210

Table 2

Mix proportions of all Formulations.

	CC	*B. safensis*	*B. pumilus*	*A.luteolus*	*Chr. Imtechense*	*C. efficiens*
Cement (Kg/m^3)	608	608	608	608	608	608
Water (Kg/m^3) 0.3 w/c	182.5	175.2	175.2	175.2	175.2	175.2
Sand (Kg/m^3)	706.8	706.8	706.8	706.8	706.8	706.8
Aggregate (Kg/m^3)	989.52	989.52	989.52	989.52	989.52	989.52
SP 0.7 % of cement	4.256	4.256	4.256	4.256	4.256	4.256
Calcium lactate (Kg/m^3)	21.28	21.28	21.28	21.28	21.28	21.28
Bacterial solution (L/m^3)	–	7.296	7.296	7.296	7.296	7.296

Table 3

BET characteristics of investigated formulations.

Formulation ID	BET Area	Pore Volume	Average Pore width
	(m^2/g)	(cm^3/g) (pores size < 50 nm)	(nm)
CC	6.19	0.69	227
B. safensis	7.3	0.59	198
B. pumilus	8.24	0.51	185
Ch. imtechense	7.13	0.53	203
A. luteolus	7.17	0.56	201
C. efficiens	7.57	0.57	210

[41]. *A. luteolus* spp. can form conglomerate small and ultrasmall cyst-like dormant cells in stress conditions [42]. The pH tolerance of *Chr. imtechense* is higher and have ability to survive harsh environment [43]. Formation of cysts owing to sigma genes is reported in *C. efficiens* as well [44].

For bacterial solution preparation, LB media was autoclaved and fresh bacterial culture was inoculated via sterilized loop. Then, broth culture was incubated overnight at 37 °C while shaking at the rate of 200 rounds per minute. Growth curves of all investigated bacterial species were recorded and displayed in Fig. 1. As, bacterial growth of each specie was different so, optical density at 0.5 was opted for current research. Bacterial growth was measured using optical density (OD) at wavelength 600 nm because this wavelength range is safer for bacterial cells [45]. The value of OD was adjusted at 0.5 using blank solution [8]. Then, the cell concentration of all bacteria solutions was adjusted at 6×10^7 cells/ml.

2.2. Concrete constituent materials

Ordinary Portland cement CEM-I conforming to ASTM C-150 having a specific gravity of 3.05 with average particle size of 5.74 μm was used [46]. Initial and final setting times of cement paste as determiend by ASTM C191 [47]. The physical and chemical properties of CEM-I are summarized in Table 1. The chemical composition of cement in oxide form was determined using X-ray fluorescence technique (XRF). Fine aggregate having a fineness modulus of 2.69 and specific gravity of 2.73 was obtained from local quary Qibla Bandi (Pakistan) confirming to ASTM C128 [48]. Coarse aggregate having maximum size of 16 mm was aquired from Margalla (Pakistan). The fineness modulus and specific gravity of coarse aggregate were 2.77 and 2.71 according to ASTM C33 [49]. Sika ViscoCrete-3110, third generation high water reducing agent, was used as super plasticizer while calcium lactate was used as food source for bacteria to avoid the formation of toxic ammonia.

2.3. Mix proportions

Six different formulations were investigated and mix proportions of tested formulations are given in Table 2. Conventional concrete formulation was labelled as CC whereas formulations containing bacteria were labelled as respective bacterial species name that was used in that particular formulation. As evident from Table 2, a constant w/c ratio of 0.3 was adjusted with super plasticizer content affixed at 0.7 % by weight of cement in all the designed recipes. In bacterial mixes, bacterial solution was used in 4 % replacement of added water however calcium lactate was used in addition mode as 3.5 % of cement weight. (see Table 3.)

2.4. Casting and testing regimes

Specimens were prepared in accordance with the standard outlined by ASTM [50]. In total 300 cylindrical (100 x200mm) and 30 cubical (50x50mm) specimens were casted in six different formulations. Specimens were demolded after 24 h of casting and subjected to immersed water curing till designated testing age.

The testing scheme was divided into four phases. In the first phase, mechanical evaluation was performed by determining compression and split tensile strength of cylindrical specimens at the curing age of 3,7,28,56 and 90 days conforming to ASTM test standards C-39 [51] and ASTM-C496/C496M standards, respectively [52]. To access load–displacement response, stress–strain curves were plotted after 270 days of curing via displacement control machine using compressive load of 0.2 MPa/second [53].

In the second phase, self-healing potential was monitored through optical microscope, image processing, ultrasonic pulse velocity test (UPV) and regain in compressive strength. For healed crack measurements, specimens were pre-cracked up to 85 % of their compressive strength for visible cracks having relatively wider crack widths for simulating real cracking conditions to analyze the self-healing performance at the specified durations 3, 7, 28, 56 and 90 days of curing and monitored for specified period of 90 days.

In order to monitor internal crack healing, pre-cracked specimens were tested in compression – to determine any regain in compressive strength after the post-cracking curing age of 90 days using Equation (1) [29]. Besides, UPV values were calculated simultaneously with crack-healed width calculations according to ASTM C597[54] and healing rate was estimated using Equation (2) [55].

$$RCS(\%) = [1 - \frac{Cu - Cr}{Cu}]100 \qquad (1)$$

where; Cu = Referenced ultimate compressive strength at 90 days, Cr = Regained compressive strength after curing of pre-cracked specimens
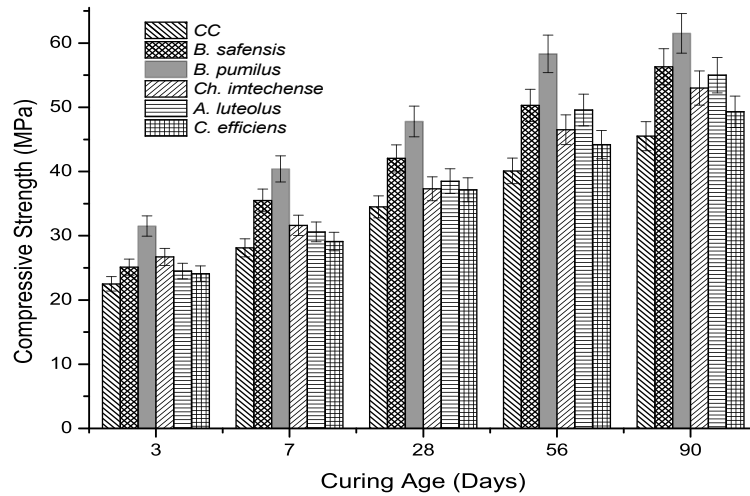
Fig. 2. Compressive strength development in bio-influenced self-healing concrete.

$$H(\%) = [1 - \frac{V}{V_0}]100 \qquad (2)$$

where; V_0 = Ultrasonic pulse velocity after pre-cracking, V= Ultrasonic pulse velocity after curing of pre-cracked specimens.

In third phase, microstructural inspection was performed using physical, micro-graphical and chemical means to trace bacterial activity alongside bacterial impact on hydration of concrete. For physical evaluation of pores sizes, BET test was conducted after 90 days of curing via procedure as per ISO 9277:2010 [56]. SEM, XRD and TG were used for forensic inspection of developed hydrates.

In phase four, the durability was accessed via sorptivity, chloride ion migration and acid attack test. Water absorption rate was measured according to ASTM C1585 using Equation (3) at the specimen age of 90 days [57]. Likewise, chloride (Cl^{-1}) migration test was performed according to NT Build 492 standard using Equation (4) after curing age of 90 days [58]. For acid attack, specimens were exposed to H_2SO_4 according to the standard ASTM C1012 / C1012M [59] and any change in length and mass were recorded at the interval of 28, 56, 90 and 135 days.

$$I_{mm} = \frac{m_t}{A.p} \qquad (3)$$

where; I_{mm} is the normalized absorption (mm), m_t is the change in mass at time (t), A is the exposed area of specimen (mm^2) and r is the density of water (0.001 g/mm^3)

$$D_{nssm} = \frac{0.0239(273 + T)L}{(U - 2)t} \left(x_d - 0.0238\sqrt{\frac{(273 + T)Lx_d}{U - 2}} \right) \qquad (4)$$

where; Dnssm is the non-steady state migration coefficient (m2/s), T is the average value of initial and final temperatures (°C), L is the thickness of specimen (mm), U is the applied voltage (V) and x_d is the average penetration depth (mm).

3. Results and discussions

3.1. Mechanical evaluation

3.1.1. Compressive strength

Compressive strength of concrete is an indicator of its resilience and aptitude against applied stresses. The measured compressive strength values of all formulations are summarized in Fig. 2. It is evident from the results that inclusion of all types of microbial solution increased the compressive strength of bio-influenced specimens in comparison to conventional concrete at all testing ages.

After curing of 3 days, CC specimens showed compressive resistance of 22.5 MPa. The compressive resistance of CC specimens kept on increasing with age owing to the on-going hydration process of cementitious matrix. At 7 and 28 days of testing, CC specimens attained strength of 28.1 MPa and 34.5 MPa, respectively. The strength gain rate was 24.8 % at 7 days with reference to 3 days strength value while 13.4 % increment was observed at 90 days strength in comparison to 56 days strength.

In case of *B. safensis* formulation, strength enhancement of 11.5 %,26.3 %, 21.8 %,25.4 % and 23.7 % with respect to CC at the testing age of 3,7,28,56 and 90 days, respectively were observed. MICP deposition is ascertained from the compressive strength development as calcite precipitation is responsible for pore refinement [60]. Moreover, the cell surface of bacteria is negatively charge and attracts positive ions that contributed to strength of the concrete [21]. It is pertinent to mention that whether bacterial cells are viable or not, they provide nucleation sites for MICP in cementitious matrix that ultimately leads into strength improvement [61].

The minimum increase in strength was observed at the age of 3 days and can be justified by the fact that initially bacteria habituated in the cementitious environment then calcite precipitation started at 7 days [62]. Actually, urea hydrolysis is accelerated reaction contributing in significant precipitation even 3&7 days of incubation as compare to this active pathway [63].

In case of *B. pumilus* specimens, the increase in compressive strength was 40 %, 43.7 %, 38.5 %, 45.4 % and 35.12 % at testing age of 3,7,28,56 and 90 days with respect to CC. Unlike *B. safensis* specimens, this formulation's rate of calcite precipitation remained same throughout. This could be attributed to the highly alkaliphilic nature of *B. pumilus* ensuing that it habituates earlier than *B. safensis*. It is pertinent to mention here that these two strains have not been investigated yet, however, 45 % and 19 % increase in compressive strength has been reported at 28 days using *Bacillus species* [60,64]. The addition of *Ch. Imtechense* into concrete specimens also improved strength but attained strength values were lower than *Bacillus species*. In comparison to CC, a maximum of 18.7 % increment in compressive strength was observed at 3 days of testing while 16.4 % improvement was observed after 90 days of testing. *Chryseomicrobium* genera belong to the Familia of *Planococcus,* but available literature lack in their calcite precipitation potential. Similarly, addition of *A. luteolus* improved compressive strength by 8.8 %,8.8 %, 11.5 %, 23.6 % and 20.8 % at designated testing age of 3,7,28,56 and 90 days with respect to CC. The rate of strength development of this bacterial specie was lower at early ages but higher at later ages. Likewise, *C. Efficiens* formulation exhibited compressive strength
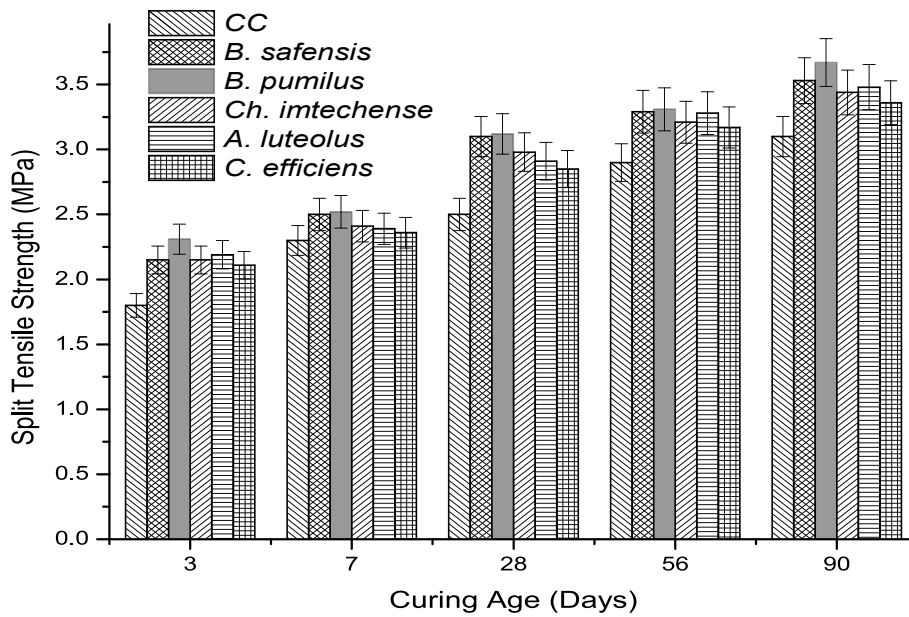
Fig. 3. Split tensile strength of bio-influenced self-healing Concrete.

improvement of 7–10 % at all designated testing ages. The strength improvement rate of this bacterial specie was lower among all SHC. It is pertinent to mention that, the feasibility of *Ch. Imtechense* and *C. Efficiens* was accessed as self-healing agent for the first time.

Overall, *Bacillus* strains depicted higher compressive strength development gain owing to their spore forming ability. Non-spore forming strains also depicted distinctively higher values as well. For example, *Ch. Imtechense* showed higher strength at early ages and *A. luteolus* showed higher strength at later ages. *C. Efficiens* showed lowest increase in strength, however, it is still appreciable.

3.1.2. Split tensile strength

The results of split tensile strength development for all formulations (conventional and bacterial) are displayed in Fig. 3. The results clearly show that all isolated calcifying bacterial strains enhanced the split tensile strength in comparison to CC.

CC specimens secured split tensile strength value of 1.8 MPa at 3 days

testing which kept on increasing owing to on-going hydration process. A maximum of 3.1 MPa of split tensile strength was attained at the age 90 days of curing. Formulation containing *B. safensis* showed an increase of 19.4 %,8.6 %,24 %,13.4 % & 13.9 % with respect to CC at respective testing age of 3, 7,28,56 & 90 days, respectively. Whereas, *B. pumilus* achieved an increase of 28.3 %,9.5 %,24.8 %,14.13 % and 18.21 % as compared to CC at all respective testing ages. In literature, a maximum of 11 % increase in split tensile strength had been reported using *Bacillus* specie. Likewise, the addition of *Ch. imtechense* also improved the split tensile strength of specimens. A maximum of 19.2 % and 10.98 % increase was observed at 28 and 90 days of testing with respect to CC. Further, formulation containing *A. luteolus* attained 21.6 %, 3.91 %,16.4,13.1 % and 12.25 % more strength than CC at all respective testing ages. Similarly, inclusion of *C. efficiens* also improved the tensile strength. A maximum of 8.3 % increment was observed after the curing age of 90 days in comparison to CC. Split tensile strength values were in agreement with compressive strength values.
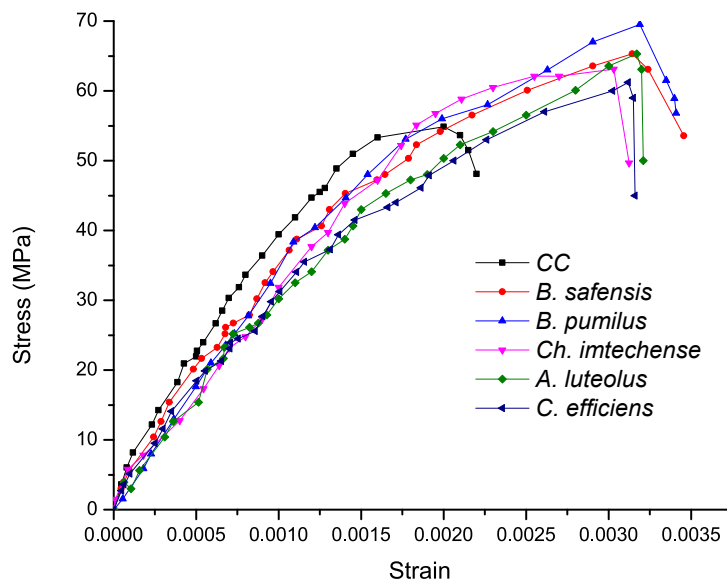

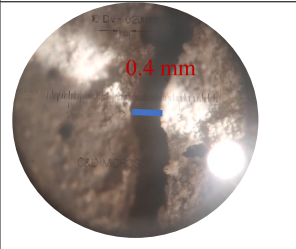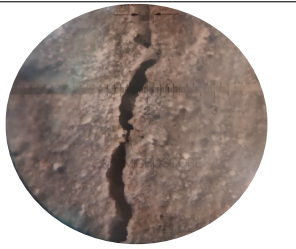**Fig. 4.** Stress–strain behavior of bio-influenced self-healing concrete.
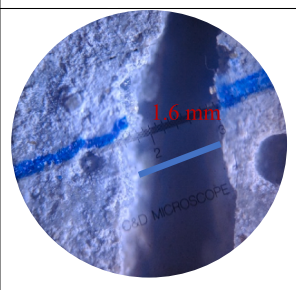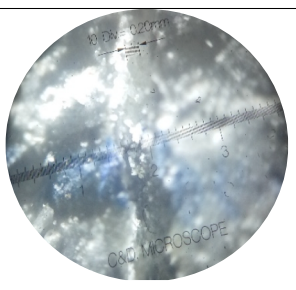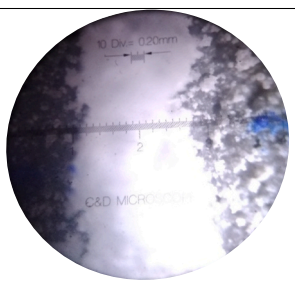
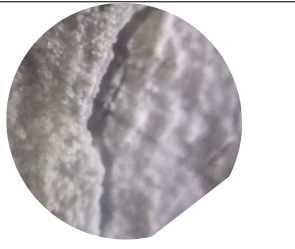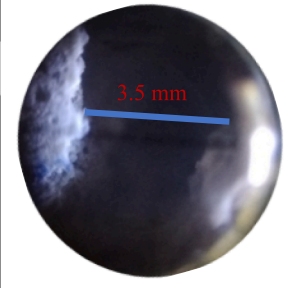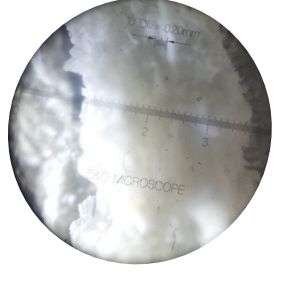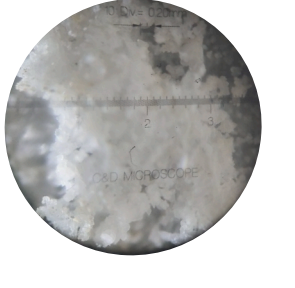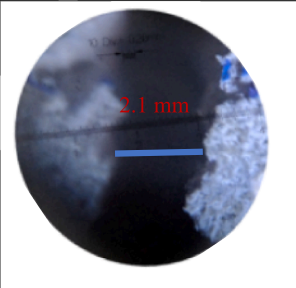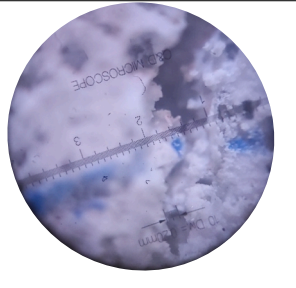| Formulation ID	Crack Width (0Day)	Crack Width (28Day)	Crack Width (90Day)
CC	0.4 mm		
B. safensis	3.5 mm		
B. pumilus	2.1 mm		
Ch. imtechense	1.6 mm		

Fig. 5. Evidence of visual crack healing of all formulations.

Overall, *Bacillus* species gave highest tensile strength values followed by *A. luteolus* and *Ch. Imtechense*. This was attributed to densification of microstructure caused by bio-mineralization [19]. *Ch. Imtechens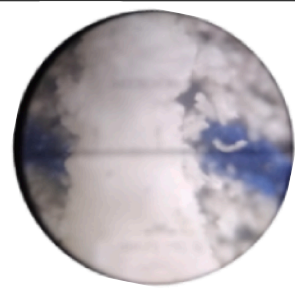e* strength gain rate was higher at early ages while *A. luteolus* attained more strength at later ages. Whereas, *C. Efficiens* depicted lowest tensile strength values among all bio-influenced formulations. Since, split tensile strength is an indication of bond strength in normal concrete matrices [65]. Bacterial cell wall having negative charge is also contributes the formation of strong interfacial zone in SHC [66]. Therefore, results obtained from test endorse the formation of adhesive bond between biosynthesized calcite and adjacent concrete matrix.

3.1.3. Stress-Strain response

Stress-strains curves of conventional concrete and bio-influenced formulations are represented in Fig. 4. It is evident from results that stress–strain response of bio-influenced formulation is better as compared to conventional concrete. This indicates that formation of MICP increased the strain capacity of the matrix. Currently, published data is silent about response of calcite precipitation in stress–strain behavior of concrete matrix. However, these results are in line with the study where crystalline admixtures were used to induce the calcite precipitation instead of microbes and improved behavior was observed [67]. All bio-influenced formulations reported the higher deformation strain than CC specimens. CC specimens had lowest strain bearing capability of 2.26 ‰. Among SHC, *B. pumilus* offered highest strain bearing aptitude of 3.3 ‰. Then, *B. safensis* and *A. luteolus* showed similar strain capability having 3.2 ‰. After them, *Ch. Imtechense* attained strain value of 3.1 ‰. Among all bio-influenced formulations *C. Efficiens* attained lowest strain value that was still higher than concrete. The strain endurance of each bacterial strain was linked with its calcite precipitation potential as each bacterial strain exhibited different calcite deposition rate [36].
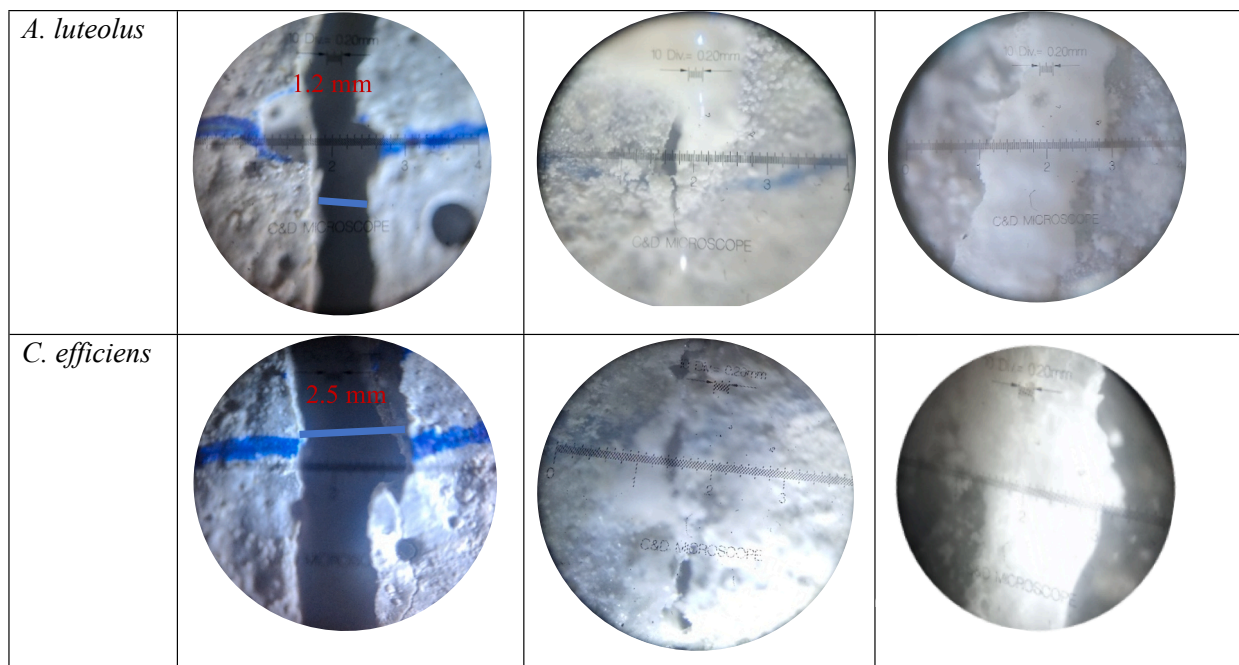
Fig. 5. (*continued*).

3.2. Healing measurements

3.2.1. Visual inspection and crack healing quantification

After post cracking of specimens, five to eight cracks of variable widths were marked on each specimen before subjected to immersed Healing. Then, these marked cracks were monitored for any crack sealing after post-cracking curing period of 28 and 90 days. Photographic imageries of maximum healed crack captured at different healing stages from same region of each formulation are given in Fig. 5. These pictures were recorded using camera put up on optical microscope, therefore scale is not visible in some pictures. It is eminent from Fig. 5 that after 28 days of post-cracking, 80 % of marked cracks were healed. Whereas, these cracks were completely healed t the age of 90 days. As illustrated from the photographs, deposition of white crystalline powder was visible inside the cracks subsequent to microbial activity in bio-influenced formulations. However, in CC specimens, cracks were partially healed having relatively lesser healing widths with nonuniform healing. Overall, *B. safensis* healed the maximum crack width of 4 mm.

For qualitative analysis of healing, average crack-healing widths were measured in millimeters (mm) based on healed response of each crack after post-cracking curing period of 28 & 90 days and result are plotted in Fig.6. It is evident from the results that addition of bio-healing agent amplified the crack healing widths at all pre-cracking periods. In CC specimens, 0.2 and 0.1 mm healing was observed when specimens were pre-cracked at 3 and 7 days after the post-cracking curing period of 28 days. Crack-healing in CC formulations can be attributed to the autogenous healing due to hydration and filling by loose particles of cracked faces[68]. The healing rate of CC specimens was depleted with increase in pre-cracking age of specimens as 0.08, & 0.05 mm crack sealing were observed at pre-cracking age of 28 and 90 days. This declined healing rate of CC specimens at later ages is indication of nonavailability of free lime owing to hardened concrete matrix. In contrast to CC, the specimens containing *B. safensis* showed average crack healing width of 0.6 and 0.5 mm at early age pre-cracking while 0.3 and 0.2 mm at later pre-cracking ages. Similarly, *B. pumilus* attained 0.5 mm and 0.4 mm crack-healing at 3 &7 days of pre-cracking and 0.25 to 0.18 mm at 28 to 90 days at pre-cracking period. Likewise, *Ch. Imtechense* attained 0.35 to 0.25 mm healing width at 3 & 28 days of pre-cracking age

whereas *A. luteolus* and *C. Efficiens* achieved 0.3 to 0.2 mm healing width at 3 & 28 days. The healing rate of bacterial formulations was declined by increasing pre-cracking age due to non-viability of microbes after such long period and denser microstructure of concrete might had crushed the bacteria.

When immersed post-cracking healing period of specimens was increased from 28 to 90 days then higher crack-healing widths were achieved (Fig.6 (b)). In CC specimens, crack healing rate was increased from 0.2 to 0.25 at 3 days of pre-cracking. Similar higher healing rate was observed in other specimens of CC which were pre-cracked at different ages. Likewise, *B. safensis* showed larger healed widths when subjected to 90 days curing by attaining 0.8 & 0.6 mm crack healing widths at pre-cracking age of 3 & 7 days. On similar pattern, *B. pumilus* attained 0.7 & 0.5 mm average crack sealing at 3 & 7 days. The healing rate of *Bacillus species* was similar at 28, 56 and 90 days of pre-cracked specimens. *A. luteolus* showed 0.5 to 0.3 mm healing rate on the interval of 3 to 90 days of pre-cracking. *Ch. imtechense* and *C. Efficiens* showed similar trends in healed widths. Conclusively, crack healed widths were higher when specimens were pre-cracked at 3& 7 days of curing age. Later on, the healed crack widths were reduced with increasing the age of pre-cracked specimen. Minimum difference in crack sealing was observed between the specimens pre-cracked at the age of 56 & 90 day. The decrease in healing rate may be attributed to formation of compact and dense microstructure developing during the early days of curing. Moreover, during initial period of healing, abundant quantity of organic nutrient was available in concrete matrix which was consumed by microorganisms to precipitate $CaCO_3$. Hence, the amount of available nutrient progressively decreased resulting in reduced rate of healing. Further, the hardened concrete matrix may crush the microbes by exerting pressure resulting into loss of viability of microbial cells.

3.2.2. Ultrasonic pulse velocity test

The internal healing of all investigated formulations was measured using equation (1) and results are displayed in Fig. 7. The specimens were cracked at the curing age of 3,7,28,56 and 90 days then subjected to moist healing for 90 days. Strong bacterial activity was evident from the results as all bio-influenced formulations showed higher healing rates than reference conventional concrete formulation. The control formulation attained 27 % healing rate when pre-cracked at 3 days of
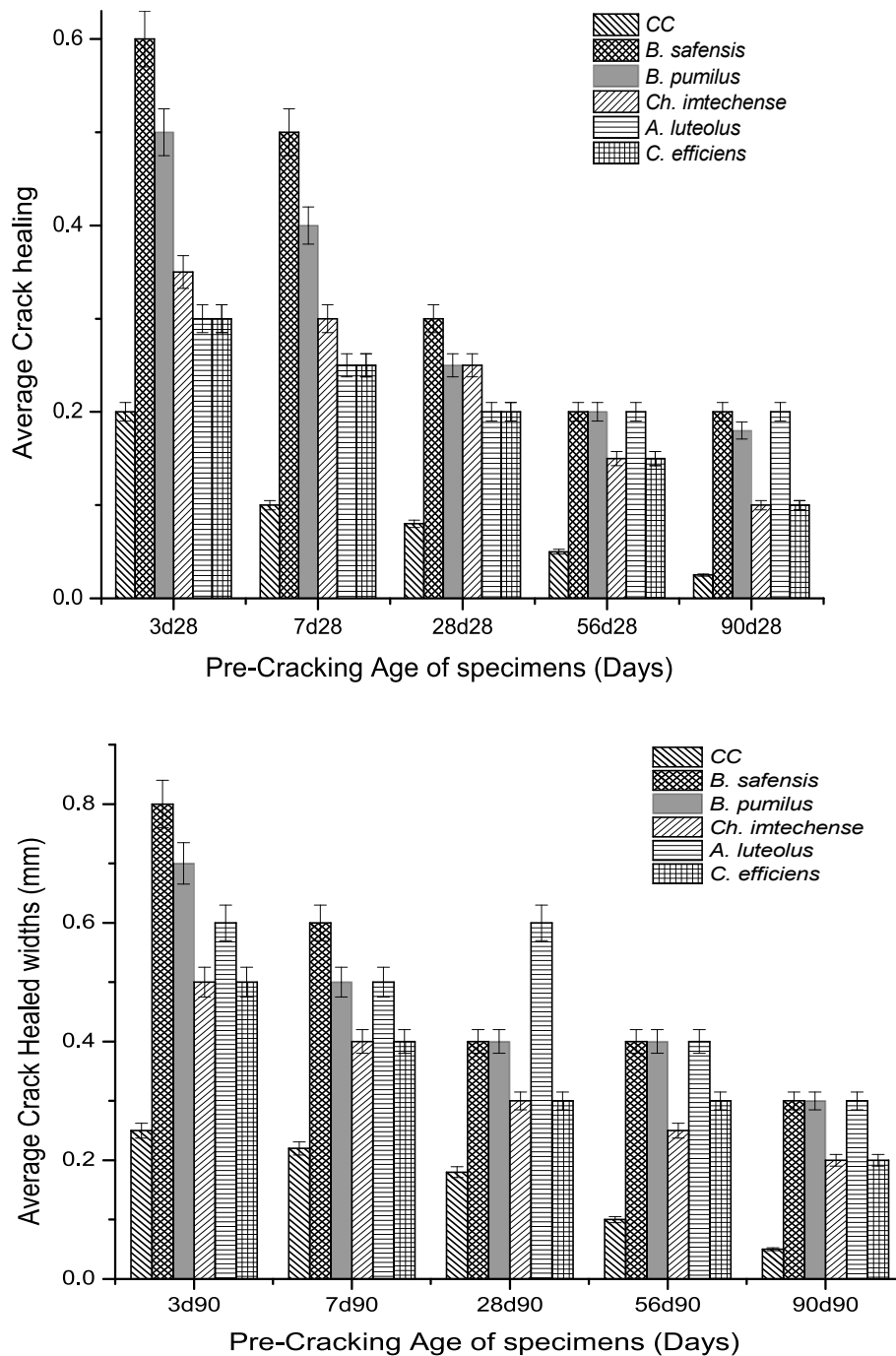
Fig. 6. (a)Average crack healing widths of specimens at the healing age of 28 days. (b) Average crack healing widths of specimens at the healing age of 90 days.

curing age. At pre-cracking age of 7 and 28 days, 19 % and 8 % healing recovery was observed. The healing rate declined with increase in the pre-cracking age of specimens owing to depleted hydration rate as discussed above. Maximum 6 % and 3 % healing rates were observed in specimens pre-racked after the curing age of 56 and 90 days.

B. safensis achieved maximum healing rate of 47 %, 27 % and 21 % at 3, 28 and 90 days of pre-cracking. Similar trend was observed in case of *B. pumilus* as 46 %, 23 % and 20 % healing rate was achieved at 3, 28 and 90 days of pre-cracking. Whereas, non-spore former, *Ch. imtechense* showed lowest healing rate 32 % and 12 % at 28 and 90 days of pre-cracking. Further, *A. luteolus* initial healing rate was lesser as compared to later age healing as 30 % and 18 % healing rate was achieved at 3 and 90 days of the pre-cracking. *C. efficiens* offered highest

healing rate at 3 and 7 days of pre-cracking after *Bacillus strains*. Overall, at later ages healing rate of *C. efficiens* was lesser followed by *Ch. imtechense*. These results are inline to those reported by [69]. UPV healing rates are in accordance to crack healing widths and compressive strength results.

3.2.3. Regained compressive strength

Regained compressive strength of pre-cracked specimens was re-evaluated to trace any healing activity inside concrete matrix using Equation (2). Specimens were pre-cracked at specified interval of 3,7,28,56 and 90 days then subjected to water curing for the period of 90 days as healing phase before re-testing. Results of CC were compared with bacterial formulations and given in Fig. 8. Isolated bacterial strains
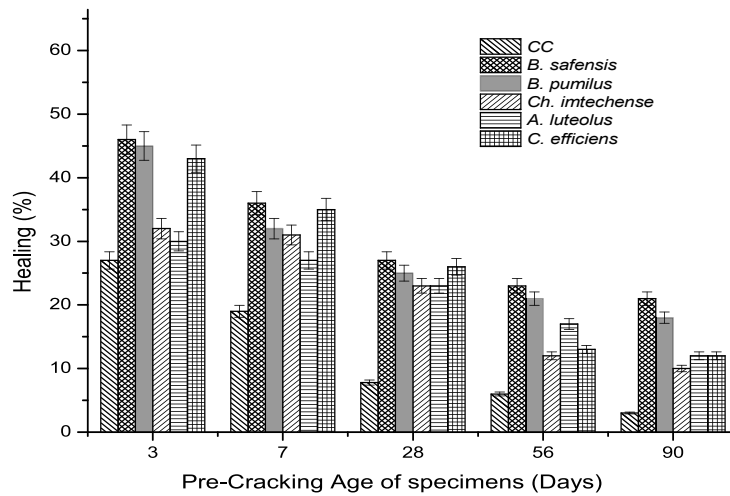
Fig. 7. Healing analysis of analyzed formulation using UPV at the healing age of 90 days.
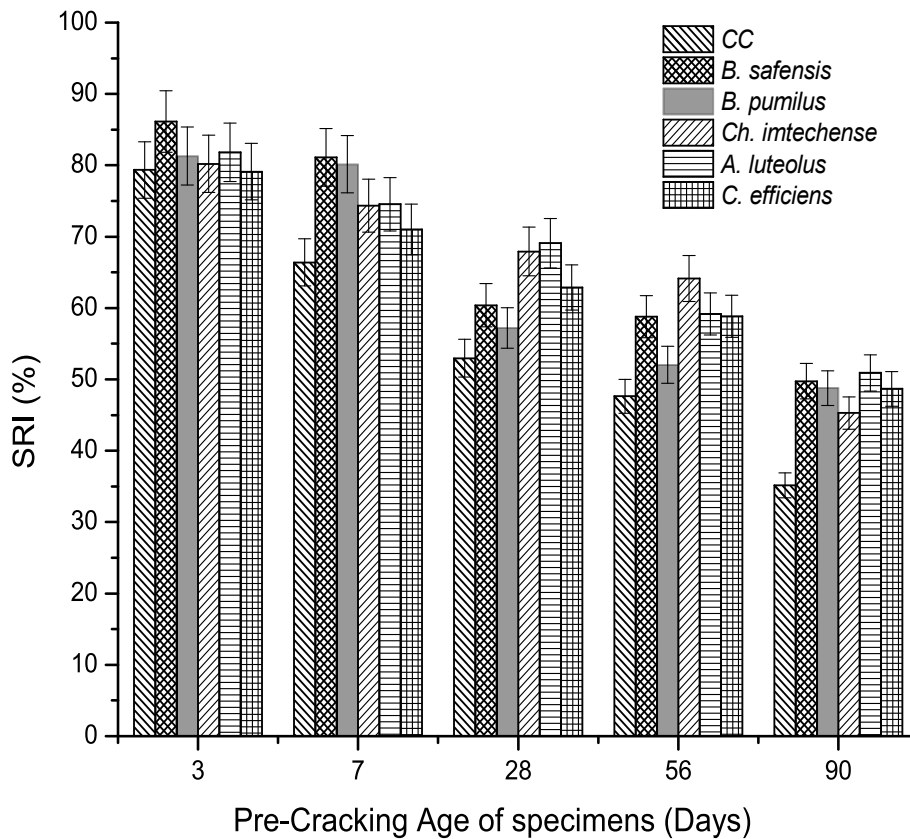

Fig. 8. SRI of analyzed formulations at healing age of 90 days.

formulations showed higher recovery than control owing to bacterial activity. CC specimens showed recovery of 79.4 % when pre-cracked at 3- days of curing age and tested after 90 days. This recovery is due to autogenous healing of cementitious systems [70]. Low percentage strength recovered in PC is due to sole natural hydration of un-hydrated cement grains and by the carbonation of calcium hydroxide to produce calcium carbonate crystal [71,72].

As pre-cracking age was increased, recovery index of CC reduced. At 90 days of pre-cracking 15 % recovery was observed in theses speci-mens. Whereas, *B. Safensis* formulation showed 86 %, 60.2 % and 49 % recovery at 3, 28 and 90 days respectively. This attributed to the highest calcification rate of precipitation of *B. Safensis* [36]. *Bacillus* strains have

been reported obtaining recovery index values of 58 % after 28 days of post-curing [60]. Similarly, *B. pumilus* attained 81 %,57.5 % and 48.5 % at 3, 28 and 90 days. Non-spore forming species of *Ch. imtechense, A. luteolus* and *C. efficiens* showed more than 80 % recovery rate on pre-cracked at 3 days. However, SRI values reduced to 45 % when pre-cracked at 90 days. it is pertinent to mention that, the values of recov-ery index of spore former and non-spore former bacterial strains were comparable. This indicated the viability of vegetative cells inside the concrete matrix. All bio-influenced formulations portrayed more strength recovery at 3 and 7 days. Then, their recovery index gradually reduced with time. The declined trend in SRI index is attributed to refinement in matrix pore structure that may crush the bacteria as
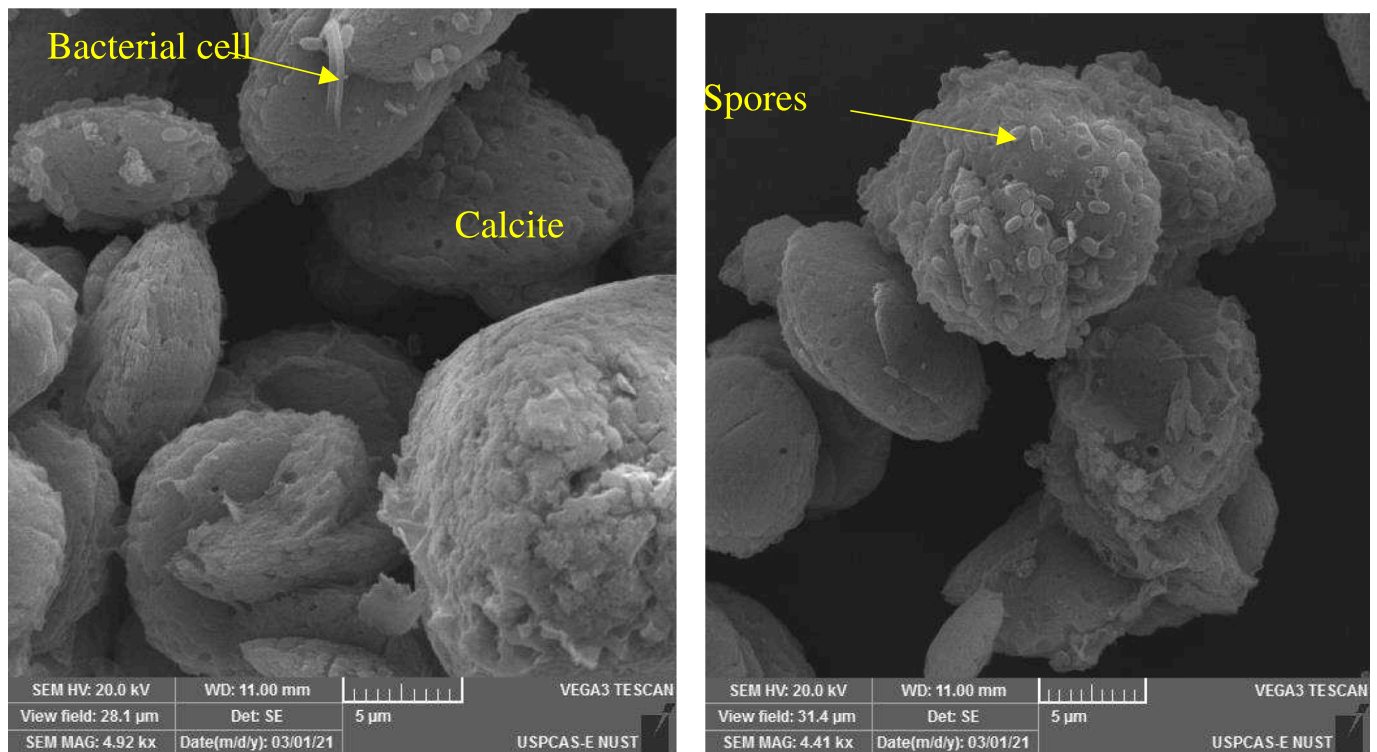
Fig. 9. SEM of precipitated healing compounds.
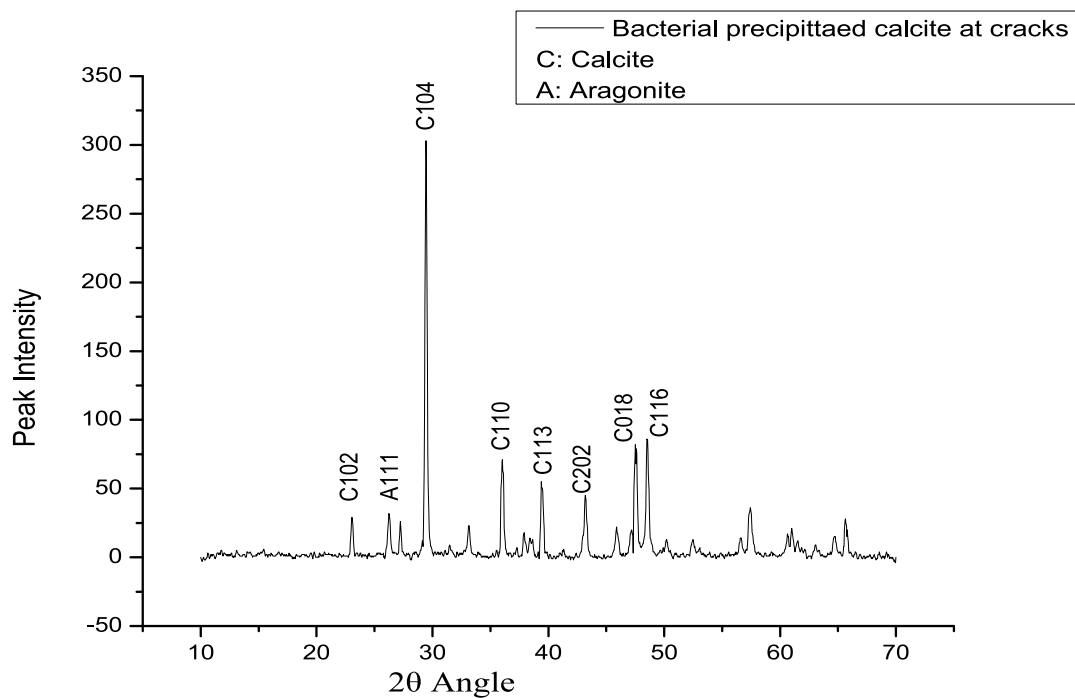
Fig. 10. XRD of precipitated healing compounds.

typical hardened matrix pore size is 1-μm [70].

3.2.4. Healing precipitate characterization

Healing precipitate was scratched from the specimen's surface carefully and characterized using SEM, XRD and TG techniques. The viability of bacteria was accessed through SEM directly and indirectly through mechanical, healing and durability analysis. The SEM

micrographs of bacteria were captured during calcite precipitation and displayed in Fig. 9. This specimen was scraped off *B. safensis* formulation. Spherical shapes (oval lens) are calcite crystals. The detail study of viability of these microbes have been discussed in this article published by the authors [36].

XRD of scratched powder confirmed it as calcite as shown in Fig. 10. That was collected from formulation *A. luteolus*. The most dominant

Fig. 11. TGA and its derivate of precipitated healing compound.
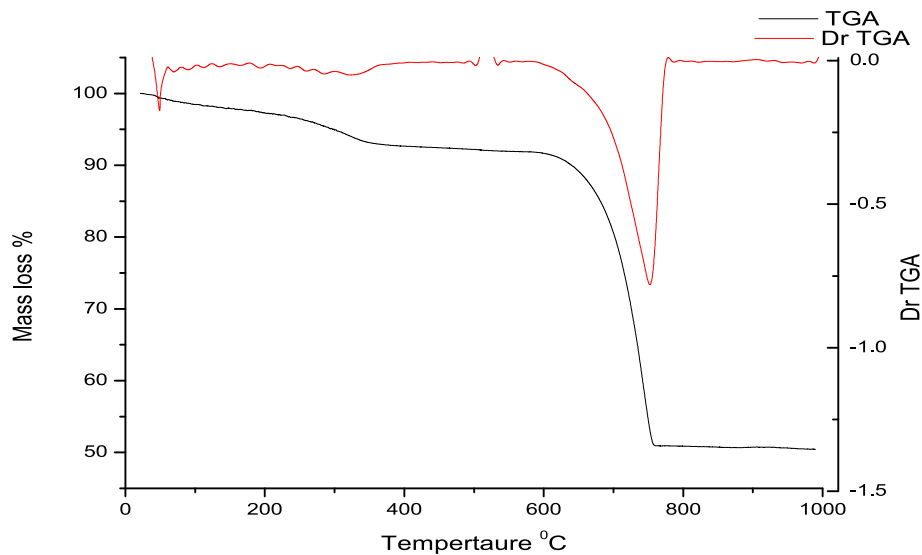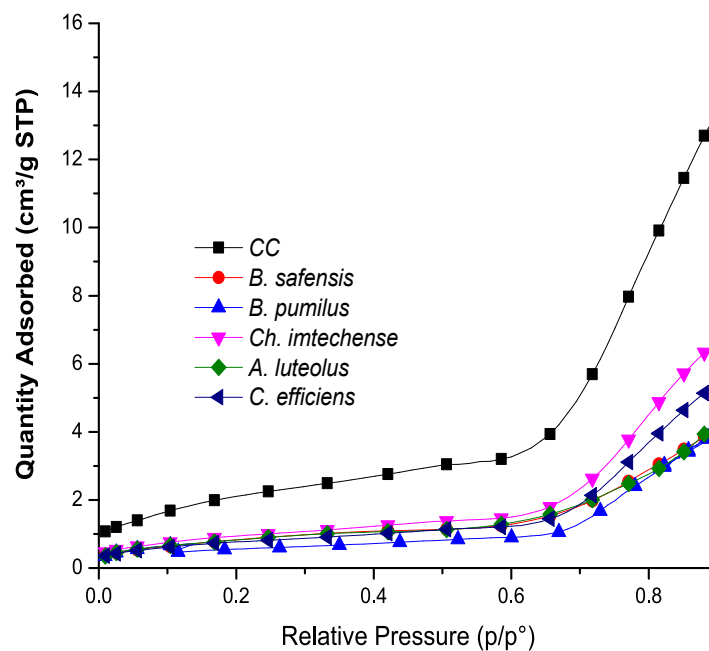

Fig. 12. BET profiles of investigated formulations.

peak was obtained at 2θ value of 29.57° which was very close to 29.3°, 2θ value of pure calcite reported by Belcher et al.[73]. Some traces of aragonite were also observed in XRD peaks.

Results obtained from thermogravimetric analysis of the healing compound (*C. efficiens)* showed 38.97 % weight loss in the specified temperature range of 650 °C to 850 °C as indicated in Fig. 11. The decomposition of $CaCO_3$ was specified in the temperature range of 600 °C-850 °C [74]. A similar trend was reported by Lors [24] when *Bacillus Specie* was used as healing agent in SHC.

3.3. Micro-Structural analysis

3.3.1. Pore size evaluation using BET

Gas adsorption techniques using BET was used to measure the pores distribution in conventional and bio-formulations. Nitrogen was used as gas source owing to its efficiency for capturing cementitious pores alignment. Results of BET analysis are tabulated in Table 2. Addition of microbes decreased the average pore diameters of concrete. Conventional concrete was having larger mean pore diameter of 227 nm. Whereas, *B. safensis* and *B. pumilus* addition reduced the average diameter to 198 nm and 185 nm as compared to conventional concrete, respectively. The inclusion of *Ch. imtechense* gave average pore diameter of 203 nm which was again relatively lesser than CC. Similarly, *A. luteolus* and *C. efficiens* also showed decrease in average pore diameters to 203 and 210 nm, respectively. The BET profiles of all formulations are displayed in Fig. 12. The results enforce the compressive strength trends of investigated formulations considering the relation between strength and density in concrete matrix. Ghosh et al., used *Shewanella* species and reduction was observed in cumulative volumes of bacterial treated samples [75]. So, calcite production consequent to bacterial activity has ability to improve the microstructure of hardened matrix. Similar findings were reported by Park where CO_2 curing was used to enhance the production of calcite [76].

CC

B. safensis

B. pumilus

Ch. imtechense
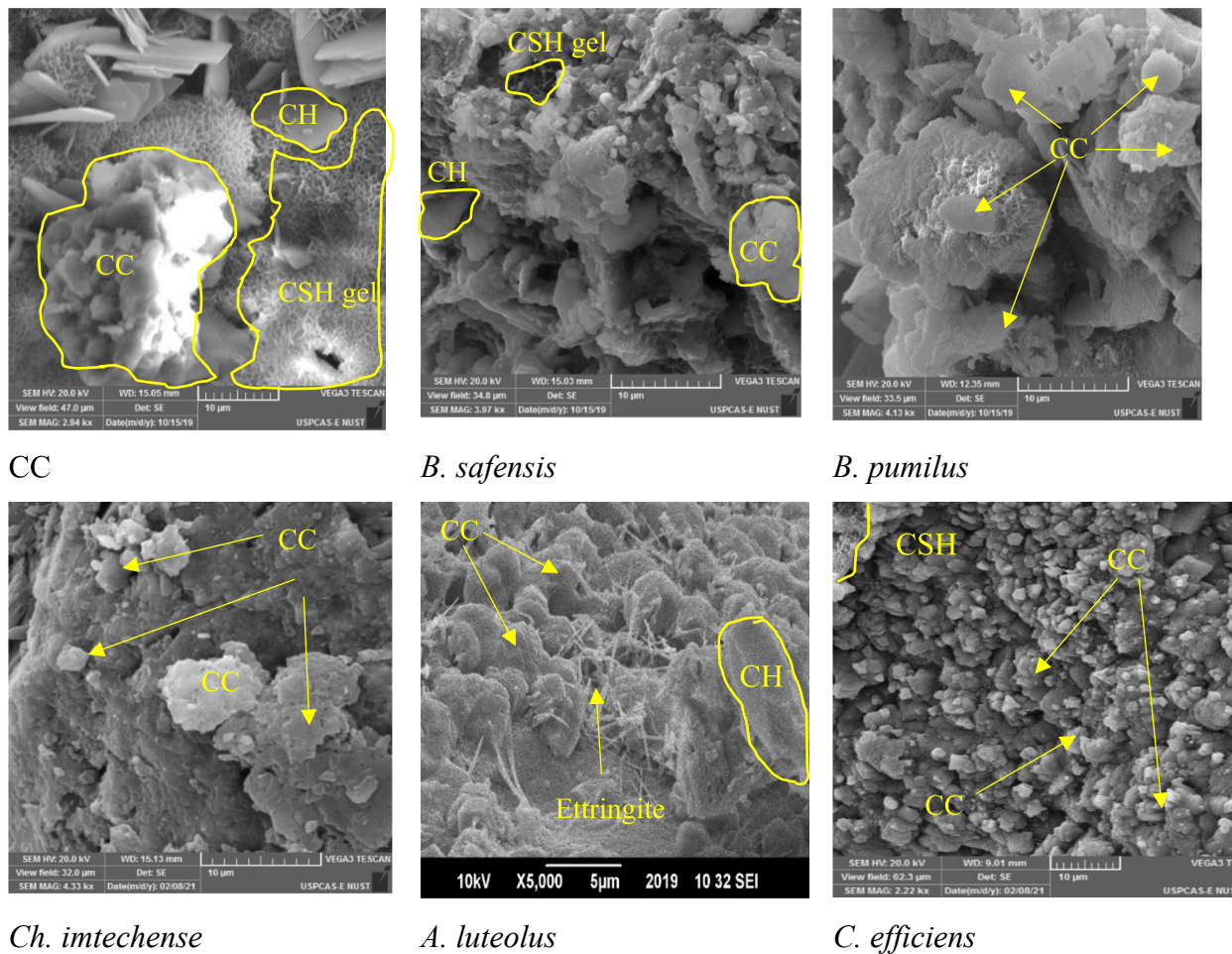
A. luteolus

C. efficiens

Fig. 13. SEM micrographs of bio-precipitate in healed cracks.

3.3.2. Microstructure analysis

The morphological investigation was performed on specimen after curing age of 90 days. The micrographs of investigated formulations are shown in Fig. 13. C—S—H gels and Ca(OH)$_2$ are prominent in reference concrete formulation. CSH gels are constituent part of cement hydrates and play a major role in strength development. Whereas Ca(OH)$_2$ having hexagonal plate-shaped crystals, being a considerably weaker phase, is responsible for providing high alkalinity of concrete environment, thereby protecting steel reinforcement against corrosion. However, high amount of calcium hydroxide (CH) may contribute to leaching, carbonation, alkali-aggregate reaction, or sulfate attack, thus deteriorating the durability of concrete structures [77]. Whereas, calcite crystals (CC) were prominent in bacteria treated formulations. These SEM images could endorse the strong bacterial activity and validate the bacterial survival for such a long period. The different morphologies of calcite crystals were precipitated by bacteria as visible in SEM micrographs. The precipitated crystals depends on type of bacterial strains as reported in literature as well [78]. The crystals precipitated by *Bacillus species* were denser and rounder in shape. However, microstructural development of *Ch. imtechense* and *A. luteolus* were somehow similar except the presence of needle like ettringite that was visible in *A. luteolus* [79]. Whereas, in *C. efficiens* treated formulation, calcite crystals were smaller in size and abundant than rest of the investigated formulation.

Further, the effect of bacteria on cement hydrates formation was analyzed via XRD that was performed against ICSD database [80]. Identified hydrates were marked on the relevant peaks as illustrated in Fig. 14. In CC formulations, portlandite, CSH gels, calcium carbonate and aluminate hydrates were present along some quartz. However,

bacterial treated specimens depicted more peaks in diffractograms subsequent to more hydrate's formations owing to bacterial activity. This confirmed the claim of more hydrates formation by Ghosh et al., in presence of bacteria [81]. As, formation of some modified CSH hydrates in presence of bacteria had been reported in literature. These hydrates phases further refined the microstructure [75,82]. Each bacterial strain influenced the cement hydrates differently. As, *B. safensis* and *C. efficiens* portrayed highest no. of peaks in spectra but more calcite was observed in *B. safensis*. Whereas *B. pumilus* gave some portlandite peaks as well. Lesser no. of peaks were seen in *Ch. imtechense* as the only confirmed peaks were of calcium carbonate and CSH gels. Further, ettringite formation in *A. luteolus* that was visible in SEM is further endorsed by XRD spectra as well.

TGA was also performed on selected formulations to diagnose the hydration product by measuring mass as function of temperature. The TGA curves are displayed in Fig. 15. More weight loss up to 7 % was observed in bacterial formulations revealing the formation of excess hydrates. In TGA curve, initial weight loss was due to evaporation and decomposition of CaSO$_4$ and CSH gels. These two quantities were lesser in CC and almost similar in both bacterial treated specimens from temperature range of (0–200 °C). More weight loss in CSH gels confirmed the formation of extra modified CSH gels in presence of bacteria. Further, weight reduction was associated with portlandite and AFM phases (200–450 °C) [79]. The wight loss of this phase was higher in *B. safensis*. CC and *C. efficiens* depicted similar values in this range. The last phase is associated with the decomposition of CaCO$_3$ (500–800 °C). CC showed lesser weight loss in this phase while both bacterial formulations depicted similar trend.
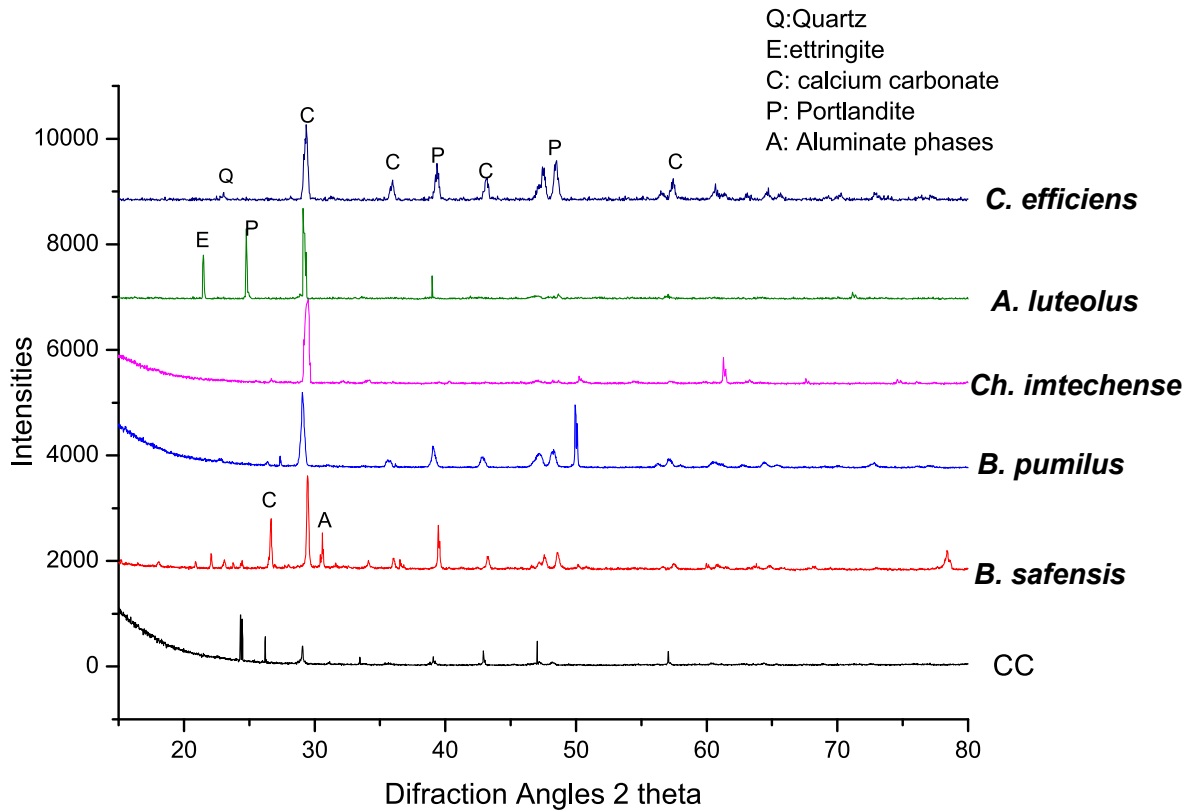
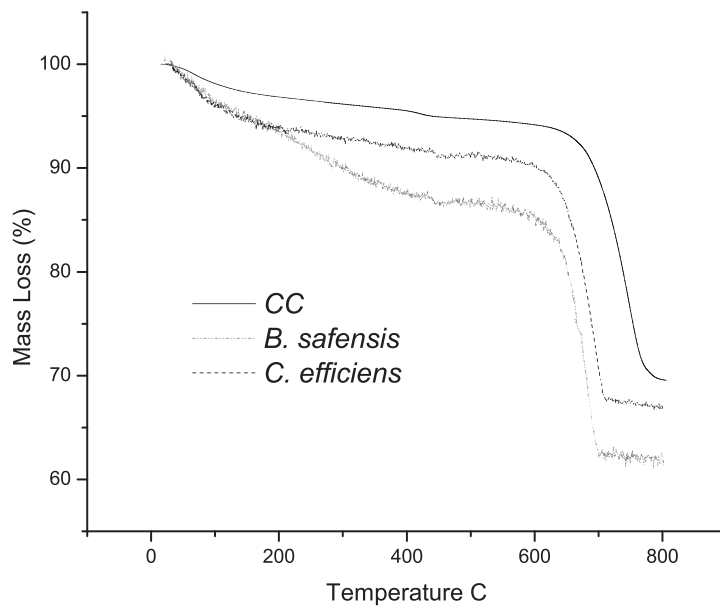**Fig. 14.** XRD Spectra of CC and bio-based concrete.

Fig. 15. TGA profiles of CC and selected bio-based formulations.

3.4. Durability assessment

3.4.1. Sorptivity

Sorptivity co-efficient of investigated formulation was calculated using Equation (3) and results are presented in Fig. 16. The water absorption rate of all bio-influenced specimens was lesser than CC specimens owing to densification of microstructure consequent of microbial activity as discussed in above sections. Rate of water absorption was higher initially then maintained at steady state. However, rate of water

absorption was found dependent on the type of bacterial strain as each strain resulted in different sopritivity index. Actually, in concrete specimens water is absorbed under suction effect through capillary pore networks [83]. As, Sorptivity co-efficient is an indication of capillary force exerted by concrete causing fluid to be drawn in microstructure. So, it gives indication of pore size diameters and no. of capillary pores. Reduction of sorptivity co-efficient evidented the disrupted capillary pore channel by bio-synthesized calcite [10]. *B. safensis* and *B. pumilus* gave 50 % and 33 % reduction in water absorption co-efficient as
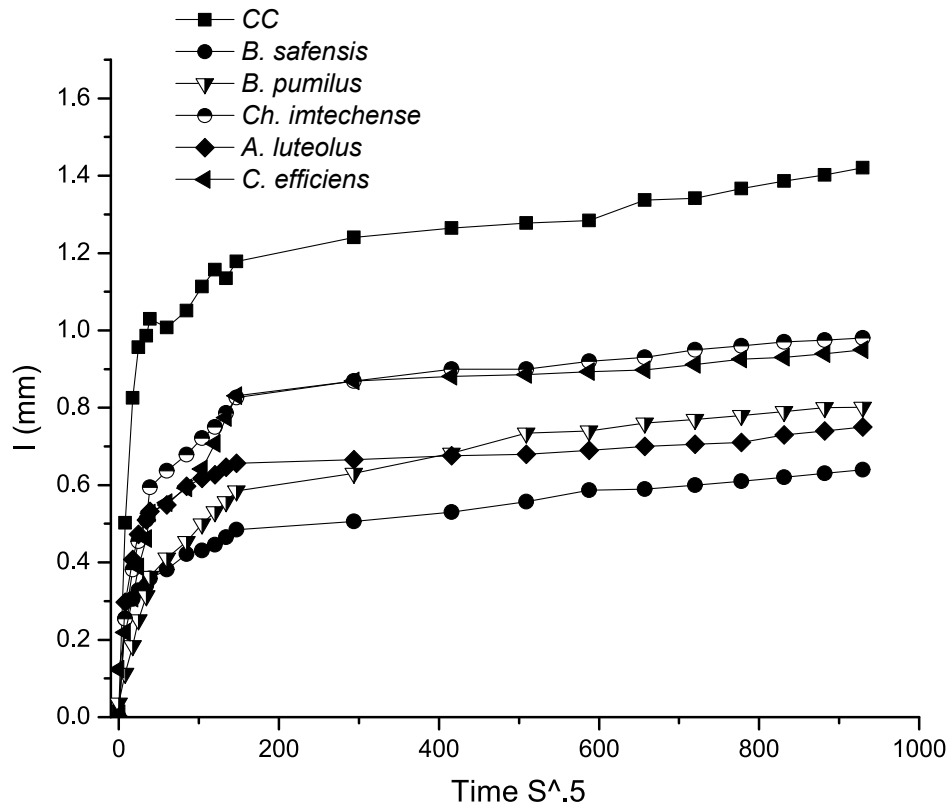
Fig. 16. Permeability co-efficient of analyzed formulations.
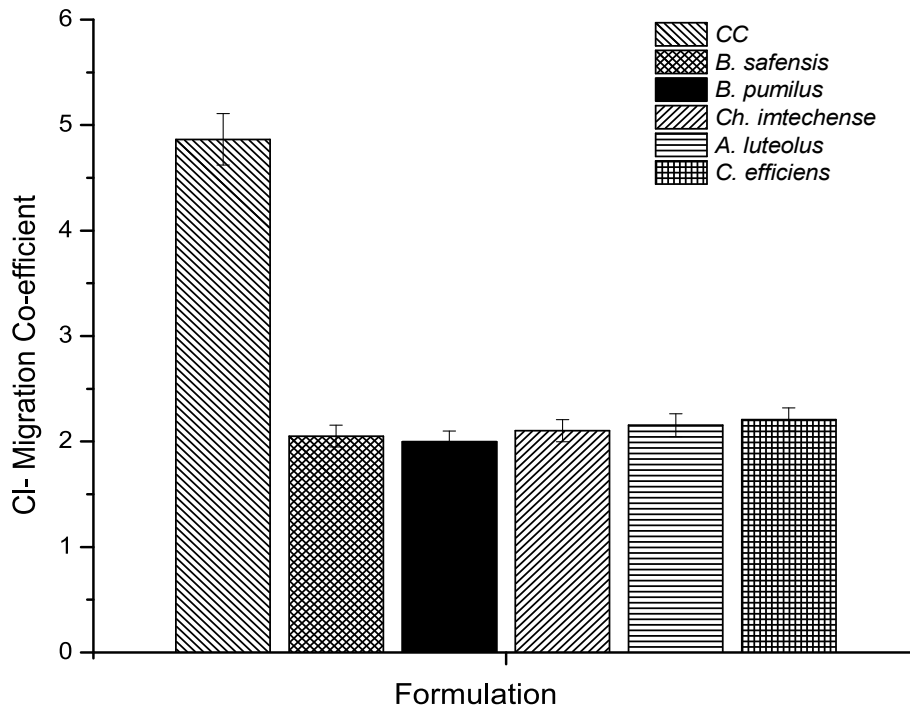
Fig. 17. Cl⁻ migration co-efficient in CC and bio-concrete.

compared to CC. Whereas, 16.4 % and 28 % reduction was endorsed in literature by using *B. subtilis* and *B. spharicus* [84,85]. During the hydration of cement, CaCO₃ precipitation on the cell wall of bacteria owing to diverse cations available in the surroundings contributed to the lesser permeability and porosity of the cement mortar [21].In another study,

50 % reduction in capillary pores discontinuity was specified using bacillus specie [86 87]. Likewise, *Ch. imtechense* induced 33 % reduction in micro-structural capillary pores with respect to CC. *A. luteolus* and *C. efficiens* attained 41.5 % reduction in capillary forces. Instead of *Ch. imtechense* formulation, other sorptivity trends are similar to the ones by

Fig. 18. Weight loss of analyzed formulations.
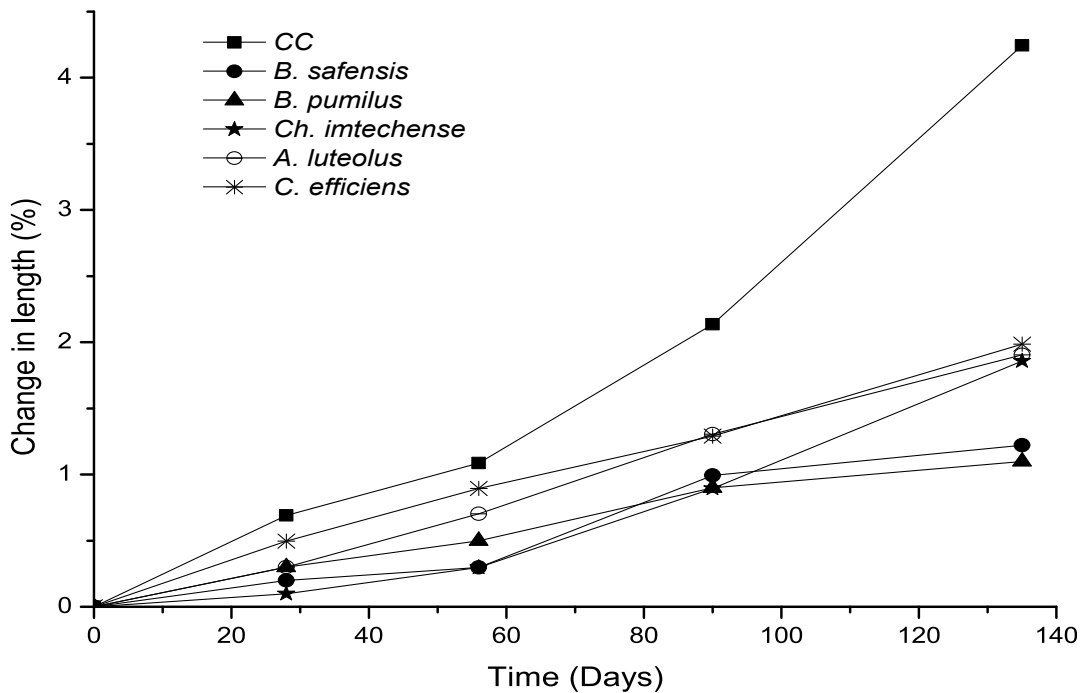
Fig. 19. Length change of analyzed formulations.

compressive strengths.

3.4.2. Chloride ion migration coefficient

The impact of bacterial strain type on chloride ion ingress aptitude of concrete is given in Fig. 17. These values were calculated using equation (4). It was evident from the results that addition of microbes greatly reduced the ingress of chloride ions. Cl⁻ ingress depends on interfacial transition and bi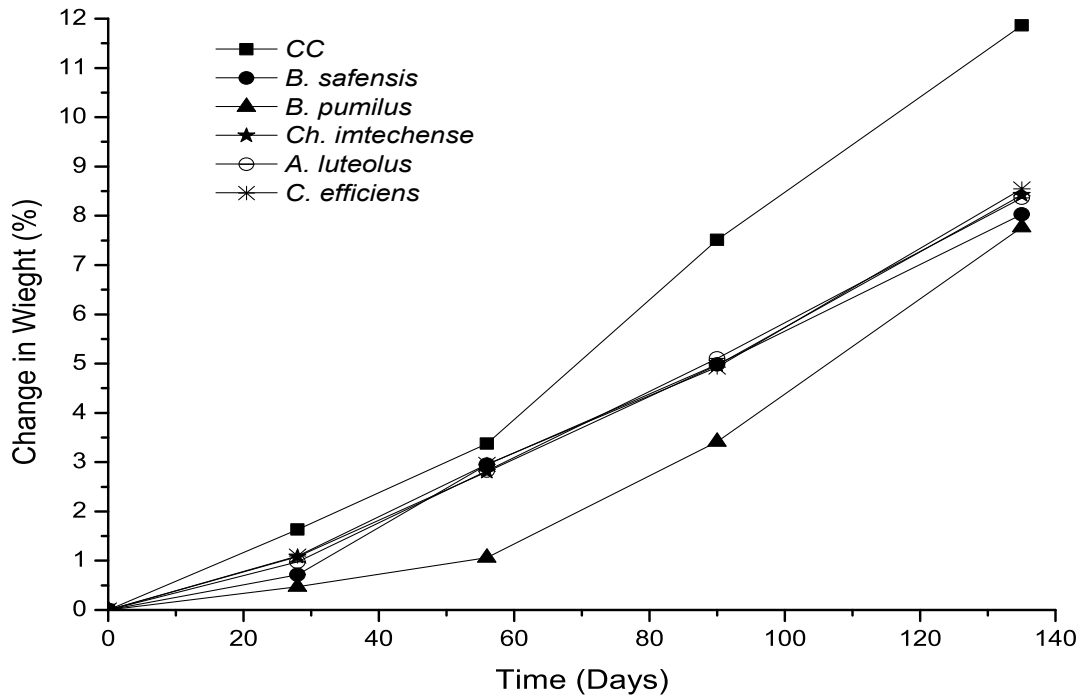nder consistency [88,89]. Interfacial zone's densification was confirmed indirectly via split tensile results. Spore-former, *B. Safensis* formulation attained 57.8 % while *B. Pumilus* attained 58.9

% reduction in Cl⁻ migration as compared conventional concrete. Whereas, 58.4 % reduction in Cl⁻ penetration is reported in the literature using *B. subtlis* [84]. Non-spore formers, *Ch. Imtechense, A. luteolus* and *C. efficiens* achieved reduction of 56.8 %, 55.7 % and 54.6 %, respectively relative to CC. Overall, bacterial concrete specimens showed 54 to 58 % reduction in Cl⁻ ingress. In already published study, 34 % reduced in Cl⁻ penetration was observed using *sporcina pasturie* [90]. High bacterial concrete resistance to Cl⁻ ingress may be attributed to working mechanism of bio-metabolic process in concrete. As, water and oxygen (O²) are culprit of Cl⁻ ingress. Whereas in bacterial concrete, the

presence of these two triggered the bacterial activity as illustrated in Eqs. (6)–(9) [91]. Moreover, less availability of portlandite in bacterial concrete renders it safe against Cl⁻ ingress [92,25,93].

$$CaC_6H_{10}O_6 + 6O_2 \rightarrow CaCO_3 \downarrow + 5CO_2 \uparrow + 5H_2O \qquad (6)$$

$$H_2O \rightarrow H^+ + 2OH^- \qquad (7)$$

$$CO_2 \uparrow + H_2O \rightarrow H^+ + HCO_3^- \rightarrow 2H^+ + CO_3^{2-} \rightarrow 2OH^- + Ca^{2+} \rightarrow CaCO_3 \quad [25]$$
$$(8)$$

$$Ca(OH)_2 + CO_2 \uparrow \rightarrow CaCO_3 + H_2O \quad [93] \qquad (9)$$
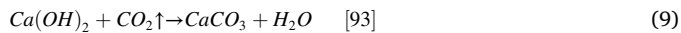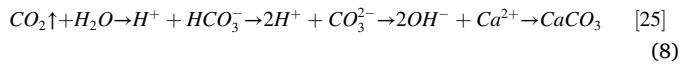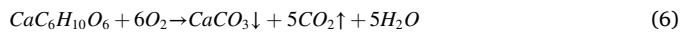
3.4.3. Sulphate attack

To understand the sulphate mechanism on bacterial concrete, any possible change in length and mass against acidic curing were monitored and illustrated in Figs. 18 and 19, respectively. This study was conducted according to the protocols given by Aliques et. Al., [83]. Moreover, H_2SO_4 was used instead of HCl owing to more aggressive nature of sulphate against bacterial concrete [94]. Length and mass changes of bacterial treated specimens were lesser than reference conventional concrete specimens. About 10.99 % weight loss was observed in control samples after 135 days of acidic curing. On the other hand, a maximum of 8.74 % weight loss was observed in bacterial concrete samples having *C. Efficiens*. A minimum of 6.7 % weight loss was observed in case of *B. Pumilus* formulation. Similar trend was given by Ozhan when *B. megaterium* was used in bacterial concrete [95]. In another study, 11.5 % and 6.5 % weight loss was observed in reference and bacterial formulation upon 60 days exposure to acid [94].

In case of length change, 4.5 % change was observed in CC formulation. Whereas, in bacterial treated concrete, weight loss was observed in the range of 0.89 % to 1.45 %. Spore-former, *Bacillus species* depicted highest resistance against acid attack. Whereas, Non-spore former *Ch. Imtechense. A. luteolus* and *C. Efficiens* offered relatively mild but similar resistance against acid (H_2SO_4). The significant resistance of bacterial treated specimens against acid attack can be attributed to formation of calcium carbonate. As, in case of sulphate attack, sulphate ions react with aluminate phases and portlandite which are present in concrete [89]. This leads to formation of gypsum which is expansive in nature and causes cracking due to internal pressure [96]. Non-availability of portlandite in bio-concrete as discussed in above section hinders this reaction. Another reason of acid resistance may be lesser permeability and strong interfacial zones in bio-concrete formulations [97,98].

4. Conclusions

In the present study, the feasibility of alkaliphilic non-spore former species of *Chryseomicrobium*, *Arthrobacter* and *Corynebacterium* as healing agent is evaluated. The proactive long-term survival of non-spore former strains in harsh concrete environment is assessed and compared with rarely explored spore former strains of *Bacillus*. This study implicit that strains of *Chryseomicrobium*, *Arthrobacter* and *Corynebacterium* have potential to be used as healing agent in SHC as their performance is comparable with *Bacillus* strains. Overall, the inclusion of all types of bacterial strains improves the mechanical resilience of self-healing concrete by maximum of 35.1 % and 18.21 % as compared to conventional concrete in compression and split tensile strength, respectively. Moreover, MICP improved the deformation response of SHC. As, deformation tolerance of bio-concrete is higher than normal concrete. Further, visual inspection of induced crack's sealing confirms the proficiency of investigated strains in surficial calcite precipitation and a maximum of 4 mm crack healing width is witnessed with average healing width of 0.8 mm. Whereas, 47 % healing effectiveness by UPV test and 86 % strength recovery index endorse the viability of bacterial strains inside alkaline cementitious environment. Additionally, refined pore network of bio-concrete instigated by strong bacterial activity is

also evident from BET and sorptivity assessment. Higher Calcite deposition in bio-concrete hydrates is forensically certified using SEM, XRD and TG analysis. This pore refinement makes bio-influenced concrete 58 % more durable against Cl⁻ penetration. Likewise, bio-concrete exhibits 33 % and 116 % resistance against mass and volumetric changes upon sulphate exposure. Certainly, the output of this study is beneficial to researchers probing for high pH resistant species having potential to thrive in cementitious environment while precipitating copious amount of calcite using environmentally friendly pathway.

It is recommended to have a detailed investigation on gene clusters of bacteria which are responsible for the calcite precipitation during the bio-healing process and its influence on hydration of cement. The impact of w/c on durability of SHC is interesting to known and recommended to investigate.

CRediT authorship contribution statement

Nafeesa Shaheen: Writing – original draft. **Rao Arsalan Khushnood:** Supervision. **Shazim Ali Memon:** Writing – review & editing. **Fazal Adnan:** Validate the result.

Declaration of Competing Interest

The authors declare that they have no known competing financial interests or personal relationships that could have appeared to influence the work reported in this paper.

Data availability

Data will be made available on request.

Acknowledgements

References

[1] H. Jonkers, Self healing concrete: a biological approach, Self Healing Materials (2008) 195–204.
[2] V. Ramakrishnan, K. Ramesh, S. Bang, Bacterial concrete, Smart Materials, International Society for Optics and Photonics, 2001, pp. 168-176.
[3] H.M. Jonkers, E. Schlangen, Crack Repair By Concrete-Immobilized Bacteria, Civil Engineering (April) (2007) 1-7.
[4] K. Van Tittelboom, N. De Belie, W. De Muynck, W. Verstraete, Use of bacteria to repair cracks in concrete, Cem. Concr. Res. 40 (1) (2010) 157–166.
[5] J. Wang, N. De Belie, W. Verstraete, Diatomaceous earth as a protective vehicle for bacteria applied for self-healing concrete, J. Ind. Microbiol. Biotechnol. 39 (4) (2012) 567–577.
[6] P. Minnebo, G. Thierens, G. De Valck, K. Van Tittelboom, N. De Belie, D. Van Hemelrijck, E. Tsangouri, A Novel Design of Autonomously Healed Concrete: Towards a Vascular Healing Network, Materials 10 (1) (2017) 49.
[7] V. Wiktor, H.M. Jonkers, Quantification of crack-healing in novel bacteria-based self-healing concrete, Cem. Concr. Compos. 33 (7) (2011) 763–770.
[8] N. Shaheen, R.A. Khushnood, W. Khaliq, H. Murtaza, R. Iqbal, M.H. Khan, Synthesis and characterization of bio-immobilized nano/micro inert and reactive additives for feasibility investigation in self-healing concrete, Constr. Build. Mater. 226 (2019) 492–506.
[9] R.A. Khushnood, S. Uddin, N. Shaheen, S. Ahmad, F. Zarrar, Bio-inspired self-healing cementitious mortar using Bacillus subtilis immobilized on nano-/micro-additives, J. Intell. Mater. Syst. Struct. (2018).
[10] S. Bhaskar, K.M. Anwar Hossain, M. Lachemi, G. Wolfaardt, M. Otini Kroukamp, Effect of self-healing on strength and durability of zeolite-immobilized bacterial cementitious mortar composites, Cem. Concr. Compos. 82 (2017) 23–33.
[11] Y. Al-Salloum, H. Abbas, Q. Sheikh, S. Hadi, S. Alsayed, T. Almusallam, Effect of some biotic factors on microbially-induced calcite precipitation in cement mortar, Saudi journal of biological sciences 24 (2) (2017) 286–294.
[12] J.W.A. van Beilen, S. Brul, Compartment-specific pH monitoring in Bacillus subtilis using fluorescent sensor proteins: a tool to analyze the antibacterial effect of weak organic acids, Front. Microbiol. 4 (2013).

[13] Y. Hu, W. Liu, W. Wang, X. Jia, L. Xu, Q. Cao, J. Shen, X. Hu, Biomineralization Performance of Bacillus sphaericus under the Action of Bacillus mucilaginosus, Adv. Mater. Sci. Eng. 2020 (2020) 6483803.

[14] T.A. Krulwich, R. Agus, M. Schneier, A.A. Guffanti, Buffering capacity of bacilli that grow at different pH ranges, J. Bacteriol. 162 (2) (1985) 768–772.

[15] E.W. Nogueira, E.A. Hayash, E. Alves, C.A.d.A., Lima,, M.T., Adorno,, G., Brucha,, Characterization of alkaliphilic bacteria isolated from bauxite residue in the southern region of minas gerais, Brazil, Brazilian Archives of Biology and Technology 60 (2017).

[16] T. Sharma, M. Alazhari, A. Heath, K. Paine, R. Cooper, Alkaliphilic Bacillus species show potential application in concrete crack repair by virtue of rapid spore production and germination then extracellular calcite formation, J. Appl. Microbiol. 122 (5) (2017) 1233–1244.

[17] M. Wu, X. Hu, Q. Zhang, D. Xue, Y. Zhao, Growth environment optimization for inducing bacterial mineralization and its application in concrete healing, Constr. Build. Mater. 209 (2019) 631–643.

[18] L.J.F. Jones, R. Carballido-López, J. Errington, Control of Cell Shape in Bacteria: Helical, Actin-like Filaments in Bacillus subtilis, Cell 104 (6) (2001) 913–922.

[19] T.H. Nguyen, E. Ghorbel, H. Fares, A. Cousture, Bacterial self-healing of concrete and durability assessment, Cem. Concr. Compos. 104 (2019), 103340.

[20] W. De Muynck, N. De Belie, W. Verstraete, Microbial carbonate precipitation in construction materials: a review, Ecol. Eng. 36 (2) (2010) 118–136.

[21] S. Luhar, I. Luhar, F.U.A. Shaikh, A review on the performance evaluation of autonomous self-healing bacterial concrete: mechanisms, strength, durability, and microstructural properties, Journal of Composites Science 6 (1) (2022) 23.

[22] S. Castanier, G. Le Métayer-Levrel, J.-P. Perthuisot, Ca-carbonates precipitation and limestone genesis—the microbiogeologist point of view, Sed. Geol. 126 (1–4) (1999) 9–23.

[23] R.R. Menon, J. Luo, X. Chen, H. Zhou, Z. Liu, G. Zhou, N. Zhang, C. Jin, Screening of Fungi for potential Application of self-Healing Concrete, Sci. Rep. 9 (1) (2019) 2075.

[24] C. Lors, J. Ducasse-Lapeyrusse, R. Gagné, D. Damidot, Microbiologically induced calcium carbonate precipitation to repair microcracks remaining after autogenous healing of mortars, Constr. Build. Mater. 141 (2017) 461–469.

[25] N. De Belie, J. Wang, Bacteria-based repair and self-healing of concrete, Journal of Sustainable Cement-Based Materials 5 (1–2) (2016) 35–56.

[26] S. Benini, W.R. Rypniewski, K.S. Wilson, S. Miletti, S. Ciurli, S. Mangani, A new proposal for urease mechanism based on the crystal structures of the native and inhibited enzyme from Bacillus pasteurii: why urea hydrolysis costs two nickels, Structure 7 (2) (1999) 205–216.

[27] S. Castanier, M.-C. Bernet-Rollande, A. Maurin, J.-P. Perthuisot, Effects of microbial activity on the hydrochemistry and sedimentology of Lake Logipi, Saline Lakes V, Springer, Kenya, 1993, pp. 99–112.

[28] N. Shaheen, R.A. Khushnood, A. Khalid, Influence of bio-immobilized lime stone powder on self-healing behaviour of cementitious composites, in: IOP Conference Series: Materials Science and Engineering, IOP Publishing, 2018, p. 062002.

[29] R.A. Khushnood, Z.A. Qureshi, N. Shaheen, S. Ali, Bio-mineralized self-healing recycled aggregate concrete for sustainable infrastructure, Sci. Total Environ. 135007 (2019).

[30] W. Khaliq, M.B. Ehsan, Crack healing in concrete using various bio influenced self-healing techniques, Constr. Build. Mater. 102 (2016) 349–357.

[31] Y. Tang, J. Xu, Application of microbial precipitation in self-healing concrete: A review on the protection strategies for bacteria, Constr. Build. Mater. 306 (2021), 124950.

[32] I. Sandalci, M.M. Tezer, Z. Basaran Bundur, Immobilization of bacterial cells on natural minerals for self-healing cement-based materials, Frontiers Built Environment 7 (2021), 655935.

[33] R. Alghamri, A. Kanellopoulos, A. Al-Tabbaa, Impregnation and encapsulation of lightweight aggregates for self-healing concrete, Constr. Build. Mater. 124 (2016) 910–921.

[34] H.S.J.Y. Wang, W. Verstraete, N. De Belie, Self-healing concrete by use of microencapsulated bacterial spores, Cem. Concr. Res. (2014) 139–152.

[35] H.J. Kim, H.J. Eom, C. Park, J. Jung, B. Shin, W. Kim, N. Chung, I.-G. Choi, W. Park, Calcium carbonate precipitation by Bacillus and Sporosarcina strains isolated from concrete and analysis of the bacterial community of concrete, J Microbiol Biotechnol 26 (2016) 540–548.

[36] N. Shaheen, A. Jalil, F. Adnan, R. Arsalan Khushnood, Isolation of alkaliphilic calcifying bacteria and their feasibility for enhanced CaCO3 precipitation in bio-based cementitious composites, Microb. Biotechnol. (2021).

[37] D.H. Bergey, J.G. Holt, P. Krieg, Bergey's manual of determinative bacteriology. 1994, Williams and Wilkins, Baltimore, MD, USA (1994).

[38] N. Shaheen, R.A. Khushnood, Bioimmobilized Limestone Powder for Autonomous Healing of Cementitious Systems: A Feasibility Study, Adv. Mater. Sci. Eng. 2018 (2018).

[39] G. Wauters, J. Charlier, M. Janssens, M. Delmée, Identification of Arthrobacter oxydans, Arthrobacter luteolus sp. nov., and Arthrobacter albus sp. nov., isolated from human clinical specimens, J. Clin. Microbiol. 38 (6) (2000) 2412–2415.

[40] P.K. Arora, A. Chauhan, B. Pant, S. Korpole, S. Mayilraj, R.K. Jain, Chryseomicrobium imtechense gen. nov., sp. nov., a new member of the family Planococcaceae, Int. J. Syst. Evol. Microbiol. 61 (8) (2011) 1859–1864.

[41] Y. Nishio, Y. Nakamura, Y. Kawarabayasi, Y. Usuda, E. Kimura, S. Sugimoto, K. Matsui, A. Yamagishi, H. Kikuchi, K. Ikeo, Comparative complete genome sequence analysis of the amino acid replacements responsible for the thermostability of Corynebacterium efficiens, Genome Res. 13 (7) (2003) 1572–1579.

[42] I.P. Solyanikova, N.E. Suzina, N.S. Egozarian, V.N. Polivtseva, N.V. Prisyazhnaya, G.I. El-Registan, A.L. Mulyukin, L.A. Golovleva, The response of soil Arthrobacter agilis lush13 to changing conditions: Transition between vegetative and dormant state, Journal of Environmental Science and Health, Part B 52 (10) (2017) 745–751.

[43] S. Waghmode, M. Suryavanshi, D. Sharma, S.K. Satpute, Planococcus species–an imminent resource to explore biosurfactant and bioactive metabolites for industrial applications, Front. Bioeng. Biotechnol. 8 (2020) 996.

[44] S. Morbach, R. Krämer, Environmental stress response of Corynebacterium glutamicum, Corynebacterium glutamicum genomics and molecular biology. Caister Academic Press, Norfolk, 2008, pp. 313–334.

[45] K. Shibata, A.A. Benson, M. Calvin, The absorption spectra of suspensions of living micro-organisms, BBA 15 (4) (1954) 461–470.

[46] A.P. Cement, ASTM C 150, Type I or II, except Type III may be used for cold-weather construction, Provide natural color or white cement as required to produce mortar color indicated 1 (1993).

[47] A. Standard, C191 Standard Test Methods for Time of Setting of Hydraulic Cement by Vicat Needle, American Society for Testing and Materials, 2008, pp. 1–8. ASTM C191–08,(C).

[48] ASTM, Standard test method for relative density (specific gravity) and absorption of fine aggregate, (2015).

[49] A. C33, ASTM C33 standard specifications for concrete aggregates, ASTM Standard Book, 2003.

[50] C. ASTM, 192, C 192M."Standard Practice for Making and Curing Concrete Test Specimens in the Laboratory (2000).

[51] A. C-39, 39, Standard test method for compressive strength of cylindrical concrete specimens, ASTM International, 2001.

[52] N. ASTM, C496/C496M-11, C, Standard test method for splitting tensile strength of cylindrical concrete specimens, 2011.

[53] H.W. Iqbal, R.A. Khushnood, W.L. Baloch, A. Nawaz, R.F. Tufail, Influence of graphite nano/micro platelets on the residual performance of high strength concrete exposed to elevated temperature, Constr. Build. Mater. 253 (2020), 119029.

[54] ASTM,, ASTM, C,, 597: Standard test method for pulse velocity through concrete, Am. Soc. Test. Mater West, Conshohocken, PA, USA, 2016.

[55] Y. Zhang, Q. Han, C. Liu, J. Sun, Analysis for critical success factors of energy performance contracting (EPC) projects in China, Industrial Engineering and Engineering Management, IEEM 2008, IEEE International Conference on, IEEE 2008 (2008) 675–679.

[56] I. Iso, 9277: 2010 Determination of the specific surface area of solids by gas adsorption–BET method, International Organization for Standardization, Geneva, 2010.

[57] A. c, Standard Test Method for Measurement of rate of absorption of water by hydraulic cement concretes Annual book of ASTM standards, American Society of Testing and Materials 2013 Pennsylvania, USA.

[58] N.B. 492, Concrete, mortar and cement-based repair materials: chloride migration coefficient from non-steady-state migration experiments, 1999.

[59] A.S.f., Testing, Materials,ASTM C1012/C1012M Standard Test Method for Length Change of Hydraulic Cement Mortars Exposed to a sulfate Solution, American Society for Testing and Materials Philadelphia, 2012.

[60] M. Rauf, W. Khaliq, R.A. Khushnood, I. Ahmed, Comparative performance of different bacteria immobilized in natural fibers for self-healing in concrete, Constr. Build. Mater. 258 (2020), 119578.

[61] S.L. Williams, M.J. Kirisits, R.D. Ferron, Influence of concrete-related environmental stressors on biomineralizing bacteria used in self-healing concrete, Constr. Build. Mater. 139 (2017) 611–618.

[62] R. Dikshit, A. Jain, A. Dey, A. Kumar, Microbially induced calcite precipitation using Bacillus velezensis with guar gum, PLoS ONE 15 (8) (2020) e0236745–e.

[63] B.J. Reeksting, T.D. Hoffmann, L. Tan, K. Paine, S. Gebhard, In-depth profiling of calcite precipitation by environmental bacteria reveals fundamental mechanistic differences with relevance to application, Appl. Environ. Microbiol. 86 (7) (2020).

[64] H. Kalhori, R. Bagherpour, Application of carbonate precipitating bacteria for improving properties and repairing cracks of shotcrete, Constr. Build. Mater. 148 (2017) 249–260.

[65] N.T. Dung, T.-P. Chang, I. Popov, Factors affecting bond strength at early age between cladding plaster and concrete substrate, European journal of environmental and civil engineering 18 (9) (2014) 1025–1041.

[66] M.G. Sohail, Z.A. Disi, N. Zouari, N.A. Nuaimi, R. Kahraman, B. Gencturk, D. F. Rodrigues, Y. Yildirim, Bio self-healing concrete using MICP by an indigenous Bacillus cereus strain isolated from Qatari soil, Constr. Build. Mater. 328 (2022), 126943.

[67] T. Chandra, Sekhara, Reddy, A. Raviteja, Macro mechanical properties of self healing concrete with crystalline admixture under different environments, Ain Shams Eng. J. 10 (1) (2019) 23–32.

[68] J. Zhang, Y. Liu, T. Feng, M. Zhou, L. Zhao, A. Zhou, Z. Li, Immobilizing bacteria in expanded perlite for the crack self-healing in concrete, Constr. Build. Mater. 148 (2017) 610–617.

[69] W. Zhong, W. Yao, Influence of damage degree on self-healing of concrete, Constr. Build. Mater. 22 (6) (2008) 1137–1142.

[70] H.M. Jonkers, Bacteria-based self-healing concrete, Heron 56 (1/2) (2011).

[71] J.H.a.S. E., A two component bacteria-based self-healing concrete. , 2nd International Conference on Concrete Repair, Rehabilitation and Retrofitting, ICCRRR, Cape Town, South Africa, 2008.

[72] M.D. Reis J, Nunes L, et al. , Evaluation of the fracture properties of polymer mortars reinforced with nanoparticles, Composite Structures (2011) 3002-3005.

[73] A.M. Belcher, X.H. Wu, R.J. Christensen, P.K. Hansma, G.D. Stucky, D.E. Morse, Control of crystal phase switching and orientation by soluble mollusc-shell proteins (1996) 56–58.

[74] V. Kasselouri, G. Dimopoulos, G. Parissakis, Decomposition of CaCO3 in the presence of organic acids, Cem. Concr. Res. 25 (5) (1995) 955–960.

[75] P. Ghosh, S. Mandal, B. Chattopadhyay, S. Pal, Use of microorganism to improve the strength of cement mortar, Cem. Concr. Res. 35 (10) (2005) 1980–1983.

[76] B. Park, Y.C. Choi, Investigation of carbon-capture property of foam concrete using stainless steel AOD slag, J. Cleaner Prod. 288 (2021), 125621.

[77] M. Krystek, D. Pakulski, V. Patroniak, M. Górski, L. Szojda, A. Ciesielski, P. Samorì, High-Performance Graphene-Based Cementitious Composites, Adv. Sci. 6 (9) (2019) 1801195.

[78] J. Xu, Y. Du, Z. Jiang, A. She, Effects of calcium source on biochemical properties of microbial CaCO3 precipitation, Front. Microbiol. 6 (2015) 1366.

[79] S.M.A. El-Gamal, F.I. El-Hosiny, M.S. Amin, D.G. Sayed, Ceramic waste as an efficient material for enhancing the fire resistance and mechanical properties of hardened Portland cement pastes, Constr. Build. Mater. 154 (2017) 1062–1078.

[80] M. Hellenbrandt, The inorganic crystal structure database (ICSD)—present and future, Crystallogr. Rev. 10 (1) (2004) 17–22.

[81] S. Ghosh, M. Biswas, B. Chattopadhyay, S. Mandal, Microbial activity on the microstructure of bacteria modified mortar, Cem. Concr. Compos. 31 (2) (2009) 93–98.

[82] V. Achal, M. Li, Q. Zhang, Biocement, recent research in construction engineering: status of China against rest of world, Adv. Cem. Res. 26 (5) (2014) 281–291.

[83] J. Aliques-Granero, T. Tognonvi, A. Tagnit-Hamou, Durability test methods and their application to AAMs: case of sulfuric-acid resistance, Mater. Struct. 50 (1) (2017) 36.

[84] C. Meera, V. Subha, Strength and Durability Assessment of Bacteria Based Self-Healing Concrete, IOSR Journal of Mechanical and Civil Engineering, (IOSR-JMCE) (2016) 1–7.

[85] T.S. Priya, N. Ramesh, A. Agarwal, S. Bhusnur, K. Chaudhary, Strength and durability characteristics of concrete made by micronized biomass silica and Bacteria-Bacillus sphaericus, Constr. Build. Mater. 226 (2019) 827–838.

[86] S. Reddy, D. Sreenivasa Rao, M. Seshagiri Rao, S. Ch, Permeation Properties of Bacterial Concrete.

[87] S. Gupta, H.W. Kua, S. Dai Pang, Healing cement mortar by immobilization of bacteria in biochar: An integrated approach of self-healing and carbon sequestration, Cem. Concr. Compos. 86 (2018) 238–254.

[88] D.P. Bentz, Influence of internal curing using lightweight aggregates on interfacial transition zone percolation and chloride ingress in mortars, Cem. Concr. Compos. 31 (5) (2009) 285–289.

[89] J.M. Marangu, J.K. Thiong'o, J.M. Wachira, Chloride ingress in chemically activated calcined clay-based cement, J. Chem. (2018 (2018).).

[90] N.H. Balam, D. Mostofinejad, M. Eftekhar, Effects of bacterial remediation on compressive strength, water absorption, and chloride permeability of lightweight aggregate concrete, Constr. Build. Mater. 145 (2017) 107–116.

[91] M. Li, X. Zhu, A. Mukherjee, M. Huang, V. Achal, Biomineralization in metakaolin modified cement mortar to improve its strength with lowered cement content, J. Hazard. Mater. 329 (2017) 178–184.

[92] J. Bai, S. Wild, B. Sabir, Chloride ingress and strength loss in concrete with different PC–PFA–MK binder compositions exposed to synthetic seawater, Cem. Concr. Res. 33 (3) (2003) 353–362.

[93] S. Mondal, P. Das, P. Datta, A.D. Ghosh, Deinococcus radiodurans: A novel bacterium for crack remediation of concrete with special applicability to low-temperature conditions, Cem. Concr. Compos. 108 (2020), 103523.

[94] R. Andalib, M.Z. Abd Majid, A. Keyvanfar, A. Talaiekhozan, M.W. Hussin, A. Shafaghat, R.M. Zin, C.T. Lee, M.A. Fulazzaky, H.H. Ismail, Durability improvement assessment in different high strength bacterial structural concrete grades against different types of acids, Sadhana 39 (6) (2014) 1509–1522.

[95] H.B. Özhan, M. Yildirim, Effects of acid and high-temperature treatments on durability of bacterial concrete, Uludağ University Journal of The Faculty of Engineering 25(3) 1421-1430.

[96] J. Monteny, N. De Belie, L. Taerwe, Resistance of different types of concrete mixtures to sulfuric acid, Mater. Struct. 36 (4) (2003) 242–249.

[97] O. Hodhod, G.A. Salama, Analysis of sulfate resistance in concrete based on artificial neural networks and USBR4908-modeling, Ain Shams Eng. J. 4 (4) (2013) 651–660.

[98] M.D. Cohen, B. Mather, Sulfate attack on concrete: research needs, Materials Journal 88 (1) (1991) 62–69.